G. Aad … P. Jackson … L. Lee … A. Petridis … N. Soni … M.J. White … et al. (ATLAS Collaboration)

Measurement of the forward-backward asymmetry of electron and muon pair-production in pp collisions at $\sqrt{s}$ = 7 TeV with the ATLAS detector

Journal of High Energy Physics, 2015; 2015(9):049-1-049-42

Originally published at:
http://doi.org/10.1007/JHEP09(2015)049

Published for SISSA by Springer

Received: *March 13, 2015*
Revised: *July 17, 2015*
Accepted: *August 10, 2015*
Published: *September 9, 2015*

Measurement of the forward-backward asymmetry of electron and muon pair-production in pp collisions at $\sqrt{s} = 7$ TeV with the ATLAS detector

JHEP09(2015)049

The ATLAS collaboration

E-mail: atlas.publications@cern.ch

Abstract: This paper presents measurements from the ATLAS experiment of the forward-backward asymmetry in the reaction $pp \to Z/\gamma^* \to l^+l^-$, with l being electrons or muons, and the extraction of the effective weak mixing angle. The results are based on the full set of data collected in 2011 in pp collisions at the LHC at $\sqrt{s} = 7$ TeV, corresponding to an integrated luminosity of 4.8 fb^{-1}. The measured asymmetry values are found to be in agreement with the corresponding Standard Model predictions. The combination of the muon and electron channels yields a value of the effective weak mixing angle of $\sin^2\theta^{\rm lept}_{\rm eff} = 0.2308 \pm 0.0005({\rm stat.}) \pm 0.0006({\rm syst.}) \pm 0.0009({\rm PDF})$, where the first uncertainty corresponds to data statistics, the second to systematic effects and the third to knowledge of the parton density functions. This result agrees with the current world average from the Particle Data Group fit.

Keywords: Hadron-Hadron Scattering

ArXiv ePrint: 1503.03709

doi:10.1007/JHEP09(2015)049

Contents

1 Introduction

The vector and axial-vector couplings in the neutral current annihilation process $q\bar{q} \to Z/\gamma^* \to \ell^+\ell^-$ lead to a forward-backward asymmetry A_{FB} in the polar angle distribution of the final state lepton ℓ^- with respect to the quark direction in the rest frame of the dilepton system. This paper presents measurements of the forward-backward asymmetry in electron and muon pairs from Z/γ^* boson decays and the extraction of the weak mixing angle by the ATLAS experiment. The results are based on the full set of pp collision data collected in 2011 at the LHC at a centre-of-mass energy of $\sqrt{s} = 7\,\mathrm{TeV}$, corresponding to an integrated luminosity of $4.8\,\mathrm{fb}^{-1}$.

The differential cross section for the annihilation process can be written at leading order as

$$\frac{\mathrm{d}\sigma}{\mathrm{d}(\cos\theta)} = \frac{4\pi\alpha^2}{3\hat{s}}\left[\frac{3}{8}A(1+\cos^2\theta) + B\cos\theta\right], \tag{1.1}$$

where α is the fine-structure constant, $\sqrt{\hat{s}}$ is the centre-of-mass energy of the quark and anti-quark, and θ is the angle between the lepton and the quark in the rest frame of the dilepton system. The coefficients A and B are functions of $\sqrt{\hat{s}}$ and of the electroweak vector and axial-vector couplings. In the case that the dilepton system has non-vanishing transverse momentum, p_{T}, the four-momentum of the incoming (anti-)quark is not known, as it is no longer collinear with the incoming beams. The impact of this effect on the asymmetry measurement is minimized by choosing a particular rest frame of the dilepton system, the Collins-Soper (CS) frame [1], in which the angle between the lepton and the quark, θ^*_{CS}, is calculated. The sign of $\cos\theta^*_{\mathrm{CS}}$ is defined with respect to the direction of the quark, which is, however, ambiguous in pp collisions. It is therefore chosen by measuring the longitudinal boost of the final-state dilepton system in the laboratory frame, and assuming that this is in the same direction as that of the quark in the initial state. This assumption leads to a fraction of events with wrongly assigned quark direction, which causes a dilution of the observed asymmetry. The probability of correct quark direction assignment increases with the boost of the dilepton system, thus reducing the dilution for dileptons produced at large rapidities. With this assumption, $\cos\theta^*_{\mathrm{CS}}$ can be written as a function of the lepton momenta in the laboratory frame,

$$\cos\theta^*_{\mathrm{CS}} = \frac{p_{\mathrm{z},\ell\ell}}{|p_{\mathrm{z},\ell\ell}|}\frac{2(p_1^+p_2^- - p_1^-p_2^+)}{m_{\ell\ell}\sqrt{m_{\ell\ell}^2 + p_{\mathrm{T},\ell\ell}^2}} \tag{1.2}$$

with

$$p_i^{\pm} = \frac{1}{\sqrt{2}}(E_i \pm p_{\mathrm{z},i}),$$

where E is the energy and p_{z} the longitudinal momentum of the lepton ($i = 1$) and anti-lepton ($i = 2$). The variables $p_{\mathrm{z},\ell\ell}$, $m_{\ell\ell}$, and $p_{\mathrm{T},\ell\ell}$ denote the longitudinal momentum, invariant mass and transverse momentum of the dilepton system, respectively. The first factor in eq. 1.2 defines the sign of $\cos\theta^*_{\mathrm{CS}}$ according to the longitudinal direction of flight of the dilepton system, as discussed above. The events with $\cos\theta^*_{\mathrm{CS}} \geq 0$ are classified as forward (F), while those having $\cos\theta^*_{\mathrm{CS}} < 0$ are classified as backward (B). The asymmetry A_{FB} is then defined as

$$A_{\mathrm{FB}} = \frac{\sigma_{\mathrm{F}} - \sigma_{\mathrm{B}}}{\sigma_{\mathrm{F}} + \sigma_{\mathrm{B}}}, \tag{1.3}$$

where σ_F and σ_B are the cross sections for the respective forward and backward configurations. At leading order, the second term in eq. 1.1, $B\cos\theta$, describes the asymmetry A_{FB}. This analysis measures A_{FB} as a function of the invariant mass of the dilepton system. The results, which are presented in section 5, include the detector-level values, as well as the corrections needed to take into account detector effects and dilution.

Several Standard Model parameters can be extracted from the dependence of the A_{FB} values on the invariant dilepton mass. One of these is the electroweak mixing angle $\sin^2\theta_{\mathrm{W}}$, which is defined at tree level as $1 - m_W^2/m_Z^2$. Depending on the renormalisation scheme, higher-order loop corrections may modify this relation. This analysis extracts the effective leptonic weak mixing angle $\sin^2\theta_{\mathrm{eff}}^{\mathrm{lept}}$ [2, 3] at the m_Z scale from the detector-level A_{FB} values.

The effective weak mixing angle is related to the electroweak vector coupling $\bar{g}_V^f$ via

$$\bar{g}_V^f = \sqrt{\rho_f}\left(T_f^3 - 2Q_f\sin^2\theta_{\mathrm{eff}}\right), \text{ with } \sin^2\theta_{\mathrm{eff}} = \kappa_f\sin^2\theta_W,$$

where the electroweak radiative corrections to the tree-level couplings are absorbed into the fermion-dependent factors κ_f and ρ_f, T_f^3 is the third component of the weak isospin and Q_f the electric charge of the fermion f. Using this definition of the effective weak mixing angle, the coupling retains its tree-level form multiplied by the additional factor $\sqrt{\rho_f}$. The relationship between the leptonic and quark $\sin^2\theta_{\text{eff}}$ can be approximated as a flavour-dependent shift in the leptonic $\sin^2\theta_{\text{eff}}$ [3]. Although the $\sin^2\theta_{\text{eff}}$ value from b-quarks differs the most from the one from leptons, only a few percent of the events in this analysis come from initial-state b-quarks. In particular, the effect of the quark $\sin^2\theta_{\text{eff}}$ on the measured A_{FB} is an order of magnitude smaller than the effect of the leptonic $\sin^2\theta_{\text{eff}}$. This analysis therefore measures the leptonic $\sin^2\theta_{\text{eff}}$, denoted by $\sin^2\theta_{\text{eff}}^{\text{lept}}$ in the following. Its value is extracted from the measured A_{FB} as a function of the invariant mass of the dilepton system by comparing it to MC predictions produced with varying values of the weak mixing angle. Details are given in section 6.

The most precise measurement of $\sin^2\theta_{\text{eff}}^{\text{lept}}$ comes from the combination of results from the LEP and SLD experiments [3]. Those studies yield an average leptonic $\sin^2\theta_{\text{eff}}^{\text{lept}} = 0.23153 \pm 0.00016$. The two most precise single measurements are extracted from the forward-backward asymmetry in b-quark final states, $A_{\text{FB}}^{0,b}$, at LEP ($\sin^2\theta_{\text{eff}}^{\text{lept}} = 0.23221 \pm 0.00029$) and from the leptonic left-right polarization asymmetry, A_{LR}, at SLD ($\sin^2\theta_{\text{eff}}^{\text{lept}} = 0.23098 \pm 0.00026$). These two values differ by approximately three standard deviations. More recently, the CDF [4] and D0 [5] experiments at the Tevatron and the CMS [6, 7] experiment at the LHC have also measured $\sin^2\theta_{\text{eff}}^{\text{lept}}$. The CDF (D0) measurement was performed using $Z \to \mu\mu$ ($Z \to ee$) events from $p\bar{p}$ collisions, and the CMS measurements were performed using $Z \to \mu\mu$ events from pp collisions. These results are compared to those from this analysis in section 6.

The value of A_{FB} at the peak of the Z/γ^* resonance ($m_{\ell\ell} = m_Z$), $A_{\text{FB}}^{0,\ell}$, can be written as a function of the asymmetry parameters A_ℓ and A_q,

$$A_{\text{FB}}^{0,\ell} = \frac{3}{4} A_q A_\ell, \tag{1.4}$$

with ℓ (q) denoting the leptons (quarks) in the final (initial) state. The parameters A_ℓ and A_q are directly related to the electroweak vector and axial-vector couplings, as described in section 6.3. The most precise measurements of the electron and muon asymmetry parameters were performed by SLD [3], yielding $A_e = 0.15138 \pm 0.00216$ and $A_\mu = 0.142 \pm 0.015$. The precision of the A_μ measurement is dominated by the statistical uncertainty, thus making it an interesting parameter to measure with the large number of $Z \to \mu\mu$ events produced at the LHC. The A_μ result from this analysis is presented in section 6.3. The determination of A_μ in the LEP/SLD results is entirely based on asymmetry measurements in electron and muon final states without any assumptions on the involved A_f. In contrast, the determination of A_μ presented here uses the Standard Model prediction of A_q.

2 The ATLAS detector

The ATLAS detector [8] is a general-purpose detector installed at the LHC [9] at CERN. The detector subsystem closest to the interaction point, the inner detector (ID), provides

JHEP09(2015)049

precise position and momentum measurements of charged particle trajectories. It covers the pseudorapidity range[1] $|\eta| < 2.5$ and provides full azimuthal coverage. The ID consists of three subdetectors arranged in a coaxial geometry around the beam axis: the silicon pixel detector, the semiconductor microstrip detector and the straw-tube transition-radiation tracker. A solenoidal magnet generates a 2 T magnetic field in which the ID is immersed.

Electromagnetic calorimetry in the region $|\eta| < 3.2$ is based on a high-granularity, lead/liquid-argon (LAr) sampling technology. Hadronic calorimetry uses a scintillator-tile/steel detector in the region $|\eta| < 1.7$ and a copper/LAr detector in the region $1.5 < |\eta| < 3.2$. The most forward region of the detector ($3.1 < |\eta| < 4.9$) is equipped with a forward calorimeter, measuring both the electromagnetic and hadronic energies using copper/LAr and tungsten/LAr modules.

A large muon spectrometer (MS) constitutes the outermost part of the detector. It consists of three large air-core superconducting toroidal magnet systems (each with eight coils): one barrel providing a field of about 0.5 T and two endcaps each providing a field of about 1 T. The deflection of the muon trajectories in the magnetic field is measured in three layers of precision drift tube chambers for $|\eta| < 2$. In higher $|\eta|$ regions ($2.0 < |\eta| < 2.7$), two layers of drift tube chambers are used in combination with one layer of cathode strip chambers in the innermost endcap wheels of the MS. Three layers of resistive plate chambers in the barrel ($|\eta| < 1.05$) and three layers of thin gap chambers in the endcaps ($1.05 < |\eta| < 2.4$) provide the muon trigger and also measure the muon trajectory in the non-bending plane.

A three-level trigger system is used to select events in real time. A hardware-based Level-1 trigger uses a subset of detector information to reduce the event rate to a design value of at most 75 kHz. The rate of accepted events is then reduced to about 300 Hz by two software-based trigger levels, Level-2 and the Event Filter.

3 Signal and background modelling

Monte Carlo (MC) simulated event samples used to model signal and background processes are generated and passed through the ATLAS detector simulation [10], based on the GEANT4 toolkit [11]. Simulated events acquire weights such that the resulting distributions match the ones observed in the data for the following variables: the average number of interactions per bunch crossing, the z coordinate of the interaction vertex, the lepton energy/momentum scale and resolution, and the trigger, identification and reconstruction efficiencies.

The Z/γ^* production is detected by the emission of charged lepton pairs, ee or $\mu\mu$. The contribution from $Z/\gamma^* \to \tau\tau$ followed by τ decays to electrons or muons is considered as background and subtracted from the signal. Signal samples are generated with

[1]ATLAS uses a right-handed coordinate system with its origin at the nominal interaction point (IP) in the centre of the detector and the z-axis along the beam pipe. The x-axis points from the IP to the centre of the LHC ring, and the y-axis points upward. Cylindrical coordinates (r,ϕ) are used in the transverse plane, ϕ being the azimuthal angle around the beam pipe. The pseudorapidity is defined in terms of the polar angle θ as $\eta = -\ln\tan(\theta/2)$.

JHEP09(2015)049

PYTHIAv6.4 [12] with the MSTW2008LO [13] parton distribution functions (PDFs) and a value of $\sin^2\theta_{\text{eff}}^{\text{lept}} = 0.232$ for the effective weak mixing angle. Final-state radiation from QED is taken into account using PHOTOS [14] in the exponentiated mode with multi-photon emission. For the $\sin^2\theta_{\text{eff}}^{\text{lept}}$ measurement, where sensitivity to PDFs is expected to be significant, additional PDF sets are also used, including one specifically prepared for this analysis, based on the ATLAS-epWZ12 PDFs [15]. Details are given in section 6. The cross section is calculated at next-to-next-to-leading order (NNLO) in the strong coupling using PHOZPR [16] with MSTW2008 NNLO PDFs. The ratio of this cross section to the leading-order (LO) cross section is the $m_{\ell\ell}$-dependent K-factor, applied to the generated signal for all plots shown in the following. However, the main observable described here (A_{FB}) is not affected by this LO-to-NNLO rescaling. The impact of higher-order corrections in α_{s} and α_{em} on A_{FB} and on $\sin^2\theta_{\text{eff}}^{\text{lept}}$ is assessed using the HORACEv3.1 [17], MCFMv6.6 [18] and POWHEGv1 [19] generators, as described in section 5. The POWHEG simulation is combined with PYTHIA 6.4 for showering and hadronization.

Background contributions containing prompt isolated electron or muon pairs are estimated using Monte Carlo simulation normalized using the best available cross section prediction at (N)NLO. The background from $Z/\gamma^* \to \tau\tau$ is also generated using PYTHIAv6.4. Diboson (WW, WZ, and ZZ) samples are generated with HERWIGv6.510 [20, 21] using the MRSTMCal PDFs [22]. Pair-production of top quarks is generated with MC@NLOv4.01 [23, 24] using the CTQE6L1 PDFs [25], combined with HERWIG for showering and hadronization.

The contributions from multi-jet and W+jets background events containing non-isolated leptons from heavy-flavour decays and hadrons misidentified as leptons are estimated using data-driven techniques, as described in section 4.3. Since the contribution from W+jets is found to be a small fraction of the multi-jet background over the whole invariant mass range, the term 'multi-jet background' is used in the following to denote the sum of these contributions.

4 Event reconstruction and selection

The analysis uses pp data collected in 2011, corresponding to an integrated luminosity of $4.8\,\text{fb}^{-1}$ for the electron channels and $4.6\,\text{fb}^{-1}$ for the muon channel. All events analysed were acquired under good operating conditions of the ATLAS detector. Events in the electron channels passed the single electron trigger, with an electron $E_{\text{T}} > 20$ or $22\,\text{GeV}$ (depending on the instantaneous luminosity). Events in the muon channel passed the single muon trigger with a muon p_{T} threshold of 18 GeV. The presence of a reconstructed collision vertex with at least three tracks with $p_{\text{T}} > 400\,\text{MeV}$ is required. For the muon channel, there is an additional requirement that the longitudinal position of this vertex be within 200 mm of the nominal interaction point.

4.1 Electron reconstruction

This analysis uses electrons in two distinct regions of the detector: the central region ($|\eta| < 2.47$) where tracking information is available, and the forward region

$(2.5 < |\eta| < 4.9)$, where the electron reconstruction relies only on information from the calorimeter. The inclusion of electrons in the forward region allows the reconstruction of events where the Z/γ^* candidates are emitted at large rapidity, thus reducing the effect of dilution due to the imperfect knowledge of the direction of the initial state quark.

For both the central and forward electrons, the reconstruction begins with identifying energy deposits in the calorimeters consistent with electromagnetic showers. Electron candidates in the central region are matched to a track reconstructed in the ID. A transverse energy requirement, $E_{\mathrm{T}} > 25\,\mathrm{GeV}$, is applied to both the central and forward candidates. Electron candidates in transition regions between the barrel and endcap calorimeters $(1.37 < |\eta| < 1.52)$ and between the endcap and forward calorimeters $(3.16 < |\eta| < 3.35)$ are excluded from this analysis.

The central candidates must satisfy either 'medium' or 'tight' identification criteria, based on shower shape and track quality variables [26] optimized for the 2011 data [27]. Forward electron candidates must satisfy similar medium quality criteria optimized specifically for forward electrons. When combining one central and one forward electron there is an additional requirement that the central electron be isolated. It is implemented by requiring that the transverse energy deposition in the calorimeter within a cone defined by $\Delta R = \sqrt{(\Delta\phi)^2 + (\Delta\eta)^2} = 0.2$ around the electron candidate be less than 5 GeV, excluding the electron candidate itself. The reconstruction efficiencies in simulated events are corrected to match the measured efficiencies [27]. Selected events consist of either two medium candidates in the central region (central-central, referred to as CC) or one tight central electron candidate and one medium forward electron candidate (central-forward, referred to as CF). In the CC electron channel, the electrons are required to have opposite charges. This requirement is not applicable in the CF electron channel, since the forward electron has no charge information. The effect of charge misidentification is found to be negligible in both the CC and CF electron channels [27].

4.2 Muon reconstruction

Muons identified as 'combined muons' by the reconstruction and identification algorithms [28, 29] are used in this analysis. They are reconstructed by associating and combining two independently reconstructed tracks, one in the ID and one in the MS. Combined muons are required to have transverse momentum $p_{\mathrm{T}} > 20\,\mathrm{GeV}$, and must lie within $|\eta| < 2.4$. The ID tracks associated with the muons must satisfy quality requirements on the number of hits recorded by each subdetector [28]. To reject muons from cosmic rays, the longitudinal coordinate of the point of closest approach of the track to the beamline is required to be within 10 mm of the collision vertex (see section 4.3). Rejection of multi-jet background is improved by requiring the muons to be isolated. The isolation parameter is the relative momentum isolation, defined as the sum of the p_{T} of all other tracks within a cone of $\Delta R = 0.2$ around the muon track, divided by the muon p_{T}: $\sum p_{\mathrm{T}}^{\mathrm{track}}/p_{\mathrm{T}}^{\mu} < 0.1$. The kinematic variables of the muons are measured by the ID, in order to minimize the impact of residual misalignments between the ID and the MS. This choice also reduces the impact of muon bremsstrahlung in the calorimeter on the measurement. Charge misidentification for muons is very low, with negligible effect on this analysis.

4.3 Event selection and background estimation

Events must contain two oppositely charged leptons in the muon and CC electron channels or one central electron and one forward electron in the CF electron channel. In the muon and CC electron channels, dilepton pairs with invariant masses up to 1000 GeV are used. In the CF electron channel, the $A_{\rm FB}$ measurement is performed only for dilepton masses up to 250 GeV, because the background dominates at larger masses, leading to sizeable systematic uncertainties.

Contributions of different background sources are estimated using either simulation or data-driven techniques. For dibosons (ZZ, WZ, WW), $Z/\gamma^* \to \tau\tau$ and $t\bar{t}$, contributions are estimated using simulation. The dominant background for the muon and CC electron channels, across the whole invariant mass range, is that due to $t\bar{t}$ events. Background from $Z/\gamma^* \to \tau\tau$ production (followed by $\tau \to \ell\nu$) populates the low end of the dilepton invariant mass distribution. For the electron channels, the multi-jet background is estimated using a combination of data-driven techniques. In the CC electron channel, the reverse identification method [30] is used for dilepton invariant masses below 125 GeV, while the fake-factor method [31], is employed for higher invariant masses. An overlap region is defined between 110 and 200 GeV, where the estimates from both methods are compared and a scale factor for the reverse identification estimate is determined using the fake-factor result. Since the CF electron channel only extends to a dilepton invariant mass of 250 GeV, only the reverse identification method is used. In the muon channel, the multi-jet background is estimated from data in a control region defined by inverting the muon isolation cut. The numbers of events in the control and signal regions observed in MC simulation are then used to transfer the data distribution from the control region to the signal region.

Figures 1 and 2 show the $m_{\ell\ell}$ and $\cos\theta^*_{\rm CS}$ distributions of events in the three channels. The total numbers of selected events are 1.2×10^6, 0.35×10^6 and 1.7×10^6 for the CC electron, CF electron and muon channels respectively. In the region close to the Z peak, the background contamination is estimated to be less than 1% for the muon and CC electron channels, and about 5% for the CF electron channel. The background contributions in the muon and CC electron channels increase to about 5% and 16% in the low- and high-mass regions, respectively. The CF electron channel has a background contamination of about 30% in the low-mass region. Agreement between data and simulation is observed within the uncertainties over the whole invariant mass range and also in the $\cos\theta^*_{\rm CS}$ distributions. These uncertainties contain both the statistical and systematic components and include the effects of multiple pp collisions occurring in the same or in neighbouring bunch crossing (pileup), energy/momentum scale and resolution, trigger efficiency, misalignment of the inner detectors, data-driven background estimates, and PDFs. Details are given in section 5.

Figure 2(c) highlights the $\cos\theta^*_{\rm CS}$ distribution for the CF electron channel to better illustrate the reduced impact of dilution: the forward-backward asymmetry is large enough to be observed directly from the plot. Some differences between data and simulation are observed in the lowest and highest bins in $\cos\theta^*_{\rm CS}$. As a cross check, the analysis was repeated excluding the bins in question and the impact on the $A_{\rm FB}$ and $\sin^2\theta^{\rm lept}_{\rm eff}$ results was found to be negligible.

JHEP09(2015)049

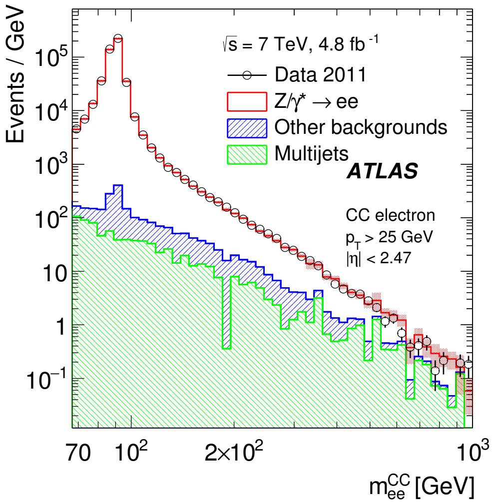

(a)

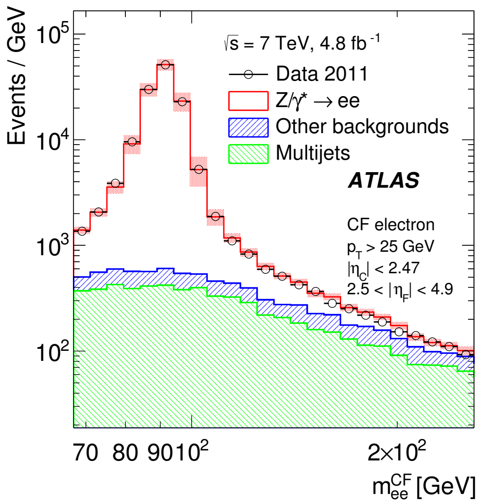

(b)

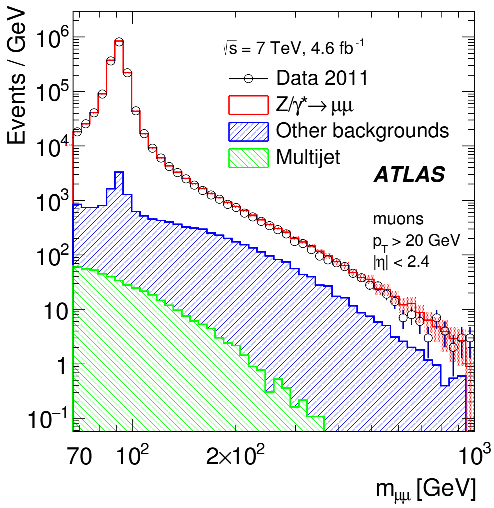

(c)

Figure 1. Dilepton invariant mass distributions obtained from the event selections described in the text, for the (a) CC electron, (b) CF electron and (c) muon channels. Data are shown by open circles and the total expectation is shown as a line with a band representing the total uncertainty (statistical and systematic added in quadrature). The data-driven estimate for the multi-jet background and the simulation-based estimates for all other backgrounds are shown by the shaded areas.

5 Measurement of A_{FB}

For each invariant mass bin, the A_{FB} value is obtained from the corresponding $\cos\theta^*_{\mathrm{CS}}$ distribution by measuring the numbers of forward and backward events:

$$A_{\mathrm{FB}} = \frac{N_{\cos\theta^*_{\mathrm{CS}}\geq 0} - N_{\cos\theta^*_{\mathrm{CS}}<0}}{N_{\cos\theta^*_{\mathrm{CS}}\geq 0} + N_{\cos\theta^*_{\mathrm{CS}}<0}}.$$

For comparison, expected A_{FB} values are calculated from both the PYTHIA and POWHEG samples described in section 3. Background contributions are subtracted from the number of forward and backward events measured at detector-level. Some background contri-

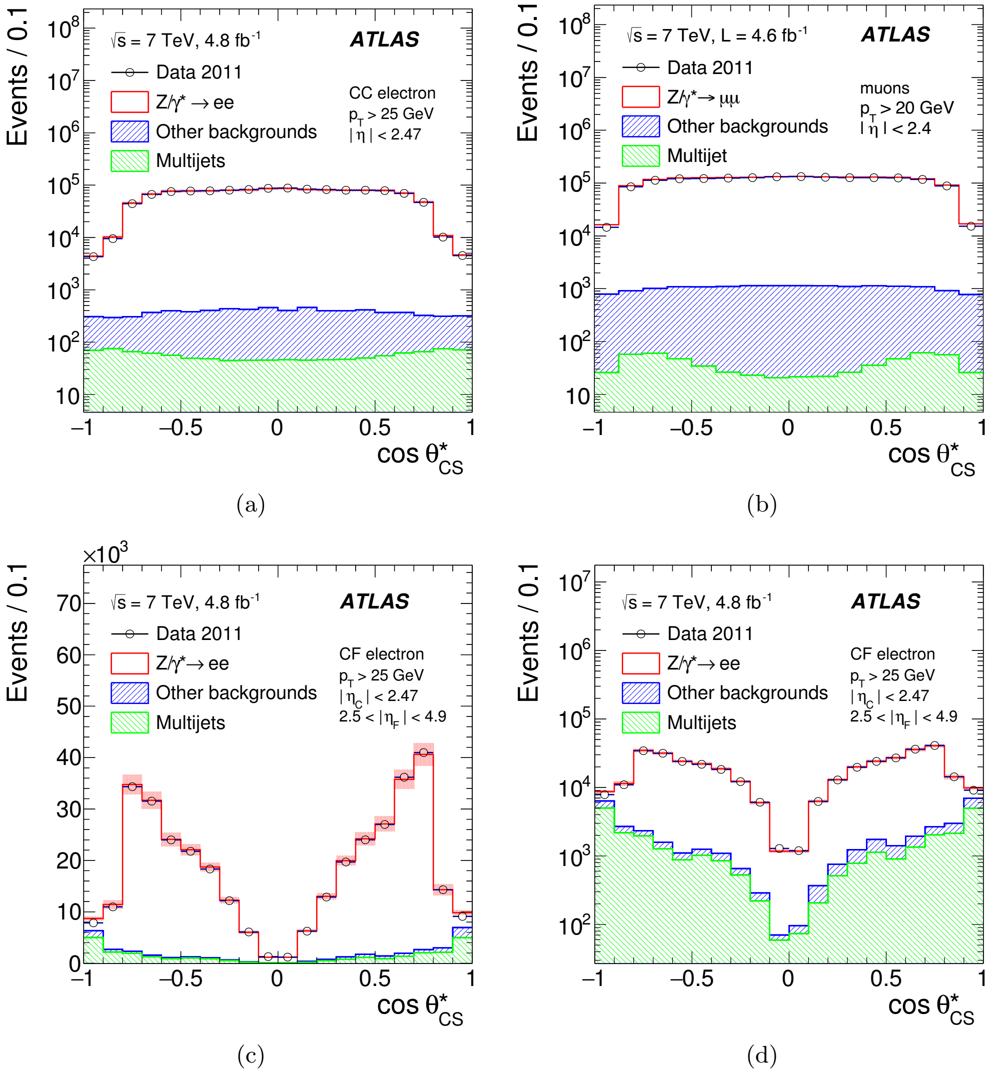

Figure 2. Distributions of the cosine of the polar angle in the Collins-Soper frame ($\cos\theta^*_{\mathrm{CS}}$) obtained from the event selections described in the text, for the (a) CC electron and (b) muon channels. The corresponding distribution for the CF electron channel is shown using both (c) a linear and (d) a logarithmic scale. Data are shown by open circles and the total expectation is shown as a line with a band representing the total uncertainty (statistical and systematic added in quadrature). The data-driven estimate for the multi-jet background and the simulation-based estimates for all other backgrounds are shown by the shaded areas.

butions, such as multi-jet events, display no asymmetry and hence dilute the measured asymmetry. Other background contributions, such as $t\bar{t}$, display an asymmetry. The detector-level asymmetry values after background subtraction ($A_{\mathrm{FB}}^{\mathrm{meas}}$) in the electron and muon channels are shown in figure 3 as a function of the invariant mass of the lepton pair.[2] Good agreement between data and simulation is observed. Figure 4 shows the same information in a narrower mass range around the Z pole.

[2]Numerical values of all results are available in HepData [32].

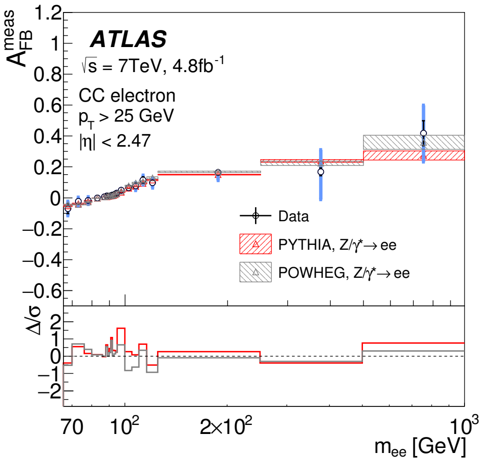

(a)

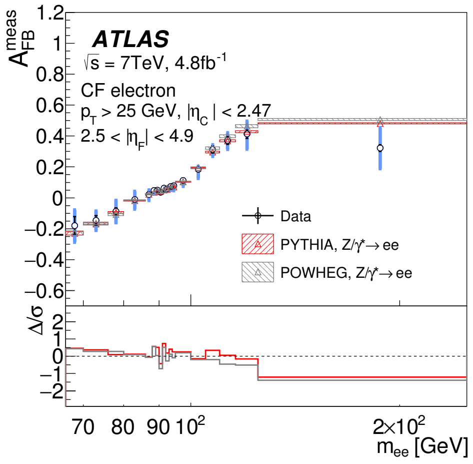

(b)

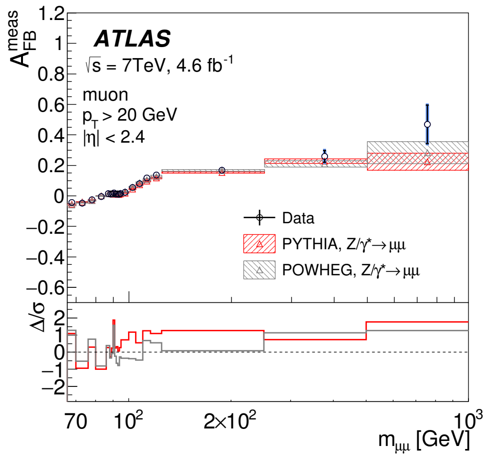

(c)

Figure 3. Detector-level forward-backward asymmetry ($A_{\rm FB}^{\rm meas}$) values as a function of the dilepton invariant mass for the (a) CC electron, (b) CF electron and (c) muon channels, after background subtraction. For the data, the black inner error bars represent the statistical component and the lighter outer error bars the total error (statistical and systematic added in quadrature). The boxed shaded regions for the MC expectations represent only the statistical uncertainty; theoretical uncertainties for MC are included in the systematic uncertainties on the data. The lower panel of each plot shows the pull value (Δ/σ) for each mass bin, where Δ is the difference between data and simulation and σ is the sum in quadrature of the data and simulation uncertainties.

The asymmetry values $A_{\rm FB}^{\rm meas}$ are unfolded from detector level to particle level ($A_{\rm FB}^{\rm obs}$), to allow comparisons with theoretical predictions. The unfolding procedure corrects for effects collectively referred to as ‘mass-bin migration’ (MBM) as described below.

- *Detector effects*: the finite resolution of the detector, as well as lepton reconstruction efficiencies, deform the measured Z/γ^* line shape and the dependence of the asymmetry values on the dilepton mass with respect to what one would measure with an ideal apparatus covering the same kinematic range.

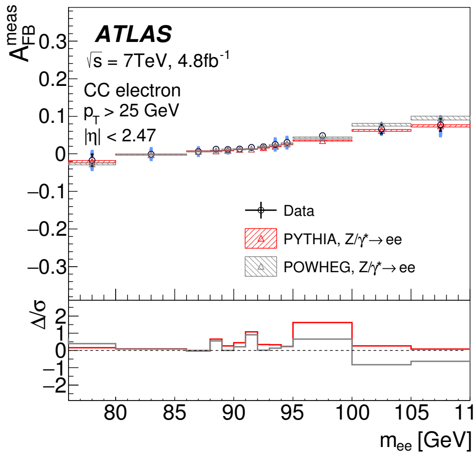

(a)

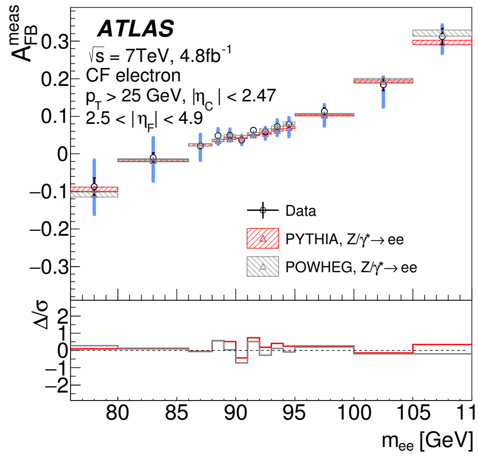

(b)

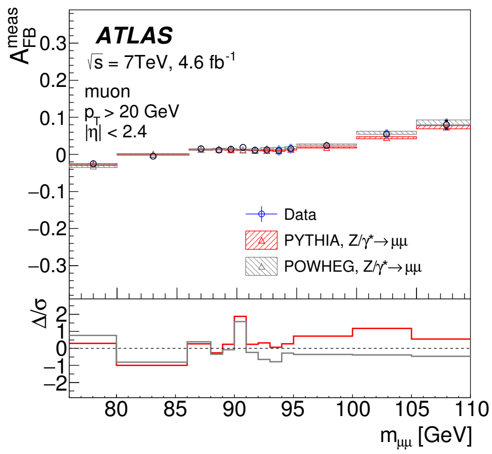

(c)

Figure 4. Detector-level forward-backward asymmetry ($A_{\mathrm{FB}}^{\mathrm{meas}}$) values as a function of the dilepton invariant mass for the (a) CC electron, (b) CF electron and (c) muon channels in a narrow region around the Z pole, after background subtraction. For the data, the black inner error bars represent the statistical component and the lighter outer error bars the total error (statistical and systematic added in quadrature). The boxed shaded regions for the MC expectations represent only the statistical uncertainty; theoretical uncertainties for MC are included in the systematic uncertainties on the data. The lower panel of each plot shows the pull values (Δ/σ, as defined for figure 3).

- *QED radiative corrections*: radiative corrections [33], or real photon emission in the final-state (FSR), deform the shape of the dilepton invariant mass distribution. This deformation is particularly pronounced below the Z peak. The events are moved from the Z peak (i.e. expected A_{FB} positive and small) towards smaller values of invariant mass, significantly reducing the magnitude of the observed A_{FB} in the region 66 GeV$< m_{\ell\ell} < m_Z$. In the high-mass region ($m_{\ell\ell} > m_Z$), the deformation due to radiative corrections is still present, but is reduced in magnitude. To account for these corrections, dileptons are unfolded to the pre-FSR state, referred to as 'Born level'.

JHEP09(2015)049

The unfolding procedure is carried out using an iterative Bayesian unfolding method [34], as implemented in the RooUnfold toolkit [35]. The response matrices are built from the PYTHIA signal sample and the number of iterations (ten) is chosen in such a way as to optimize the result of closure tests on simulated samples. Additional checks are performed to ensure that the use of the PYTHIA LO generator for the unfolding does not bias the result. Since FSR is a significant correction, an alternative real-photon emission generator is investigated, using a simulated sample generated with SHERPA [36], which uses a module called PHOTONS++ [37] for higher-order QED corrections. The impact of NLO electroweak (EWK) corrections on the response matrix are estimated by reweighting the PYTHIA simulation to the prediction from the HORACE MC event generator and redoing the unfolding. In order to estimate NLO QCD effects on the $A_{\rm FB}^{\rm obs}$ values, a test is performed using a simulated POWHEG sample as pseudo-data and unfolding the asymmetry values using the PYTHIA-derived response matrices. These studies all show that any biases are much smaller than the present statistical uncertainties of the measurement.

The systematic uncertainties on $A_{\rm FB}^{\rm obs}$ have contributions from the sources discussed in the following.

- *Unfolding uncertainty*: estimated using a partially data-driven method. A set of weights is derived as a function of $m_{\ell\ell}$ and $\cos\theta^*_{\rm CS}$ to reweight the $A_{\rm FB}^{\rm meas}$ values from simulation to the one observed in data. These weights are applied to the generator-level asymmetry values. The response matrix used in the unfolding is applied to the resulting values to fold and subsequently unfold them. Particular care is taken to make the matrices used for the folding and the unfolding statistically independent. The generator-level $A_{\rm FB}$ dependence on $m_{\ell\ell}$ is compared before and after the fold-unfold operation, and the difference is taken as an estimate of the uncertainty introduced by the unfolding.

- *Uncertainty due to finite size of the simulated event samples*: the statistical uncertainty on the response matrices is propagated through the unfolding procedure.

- *Multi-jet background modelling*: in the CC electron channel, the difference between the two background estimation methods described in section 4.3 is taken as the systematic uncertainty and is found to be negligible with respect to other uncertainties. In the CF electron channel, this uncertainty is estimated by comparing templates based on different electron isolation requirements. For the muon channel, the impact of this background (and its uncertainty) is negligible.

- *Other experimental systematic uncertainties*: these include the impact of pileup and of detector alignment, as well as energy/momentum scale and resolution, and trigger and reconstruction efficiencies. The associated systematic uncertainties are estimated following the prescriptions in refs. [26, 28, 38]. The uncertainties related to energy scaling and resolution are among the largest contributions to the total error in all three channels, since they result in both a shifting and a broadening of the invariant mass peak, causing events to migrate between mass bins.

CC electrons			
Uncertainty	66–70 GeV	70–250 GeV	250–1000 GeV
Unfolding	$\sim 1\times 10^{-2}$	$(2–5)\times 10^{-3}$	$\sim 4\times 10^{-4}$
Energy scale/resolution	$\sim 7\times 10^{-3}$	$(0.5–2)\times 10^{-3}$	$\sim 2\times 10^{-2}$
MC statistics	$\sim 5\times 10^{-3}$	$(0.1–1)\times 10^{-3}$	$(3–20)\times 10^{-3}$
PDF	$\sim 2\times 10^{-3}$	$(1–8)\times 10^{-4}$	$(0.7–3)\times 10^{-3}$
Other	$\sim 1\times 10^{-3}$	$(0.1–2)\times 10^{-3}$	$(5–9)\times 10^{-3}$
CF electrons			
Uncertainty	66–70 GeV	70–250 GeV	250–1000 GeV
Unfolding	$\sim 2\times 10^{-2}$	$(0.5–2)\times 10^{-2}$	—
Energy scale/resolution	$\sim 1\times 10^{-2}$	$(0.5–7)\times 10^{-2}$	—
MC statistics	$\sim 1\times 10^{-2}$	$(1–7)\times 10^{-3}$	—
Background	$\sim 3\times 10^{-2}$	$(0.5–1)\times 10^{-2}$	—
PDF	$\sim 4\times 10^{-3}$	$(2–6)\times 10^{-4}$	—
Other	$\sim 1\times 10^{-3}$	$(1–5)\times 10^{-4}$	—
Muons			
Uncertainty	66–70 GeV	70–250 GeV	250–1000 GeV
Unfolding	$\sim 1\times 10^{-2}$	$(1–4)\times 10^{-3}$	$\sim 5\times 10^{-4}$
Energy scale/resolution	$\sim 8\times 10^{-3}$	$(3–6)\times 10^{-3}$	$\sim 5\times 10^{-3}$
MC statistics	$\sim 5\times 10^{-3}$	$(0.1–1)\times 10^{-3}$	$(2–30)\times 10^{-3}$
PDF	$\sim 2\times 10^{-3}$	$(1–8)\times 10^{-4}$	$(0.3–3)\times 10^{-3}$
Other	$\sim 1\times 10^{-3}$	$(0.5–1)\times 10^{-3}$	$(3–10)\times 10^{-3}$

Table 1. Absolute systematic uncertainties on the $A_{\mathrm{FB}}^{\mathrm{obs}}$ values, after unfolding for mass-bin migration. Approximate values in three invariant mass intervals are given.

- *PDF uncertainties*: the CT10 PDF set [39], which provides a reliable uncertainty estimate and is widely used in ATLAS, is also used here to estimate the PDF uncertainty. Its eigenvectors are used and the result quoted at 68% confidence level. For each error set, the MC signal sample is reweighted, the response matrices are recalculated and the unfolding is repeated. This contribution is found to be small when unfolding only mass-bin migration effects.

The magnitudes of the systematic uncertainties on the $A_{\mathrm{FB}}^{\mathrm{obs}}$ values are summarized in table 1, for three invariant mass regions. Figure 5 shows the $A_{\mathrm{FB}}^{\mathrm{obs}}$ values obtained from leptons unfolded to Born level for all three channels. Expectations from PYTHIA and POWHEG are in good agreement with the measured values, as illustrated in the pull distribution at the bottom of each plot.

JHEP09(2015)049

5.1 Correcting for dilution

A similar unfolding procedure is used to further correct the $A_{\mathrm{FB}}^{\mathrm{obs}}$ values to remove dilution effects, which occur when the wrong choice is made for the direction of the quark. The unfolding for dilution and the extrapolation from the detector acceptance to the full phase space are performed using the PYTHIA signal sample, where the description of the initial state allows a straightforward definition of the polar angle of the lepton with respect to the quark. The fully corrected asymmetry values for dileptons at the Born level $A_{\mathrm{FB}}^{\mathrm{cor}}$ are shown in figure 6. The magnitude of the correction is larger than in the previous unfolding step. In addition, the contribution from the PDFs becomes the dominant systematic uncertainty. Good agreement is observed in general between the measured and predicted values. The muon channel measurement exhibits a discrepancy with respect to the PYTHIA prediction for masses above the Z boson mass, where the measured asymmetry is consistently larger than the prediction. This effect could not be explained by the analysis procedure and might be a feature of the simulation.

6 Measurement of $\sin^2\theta_{\mathrm{eff}}^{\mathrm{lept}}$

The extraction of the effective weak mixing angle ($\sin^2\theta_{\mathrm{eff}}^{\mathrm{lept}}$) from the detector-level asymmetry values ($A_{\mathrm{FB}}^{\mathrm{meas}}$) is presented here.

Within the region of interest ($0.218 \leq \sin^2\theta_{\mathrm{eff}}^{\mathrm{lept}} \leq 0.236$) 17 MC simulated samples were generated with varying values of $\sin^2\theta_{\mathrm{eff}}^{\mathrm{lept}}$. The generator used for the templates is PYTHIA, which allows the value of $\sin^2\theta_{\mathrm{eff}}^{\mathrm{lept}}$ to be tuned without changing m_Z. Within the range of the $\sin^2\theta_{\mathrm{eff}}^{\mathrm{lept}}$ variations, the Z boson line shape remains unchanged in the generated samples. From the generator-level information in the samples, weights are calculated, in bins of $m_{\ell\ell}$ and $\cos\theta^*_{\mathrm{CS}}$, to transform the $A_{\mathrm{FB}}^{\mathrm{meas}}$ values to the ones expected (A_{FB}^{rew}) for a different value of $\sin^2\theta_{\mathrm{eff}}^{\mathrm{lept}}$. The reweighting technique is validated on simulated samples. For each channel, the A_{FB}^{rew} values obtained from the reweighted datasets are compared to those obtained from the data, using a χ^2 test over the mass range 70–250 GeV, taking statistical and systematic uncertainties into account. The mass range has been optimized for the maximum sensitivity and stability of the measurement. A parabola is fitted to the resulting distributions of χ^2 values for each channel independently. The minimum of the parabola yields the $\sin^2\theta_{\mathrm{eff}}^{\mathrm{lept}}$ result. The χ^2/ndf value at the minimum is 22.4/16 for the CC electron channel, 21.9/16 for the CF electron channel and 22.6/16 for the muon channel. The fit results are found to be stable with respect to the invariant mass range over which the template comparisons are performed, as well as with respect to the $\sin^2\theta_{\mathrm{eff}}^{\mathrm{lept}}$ range over which the χ^2 is minimized.

As discussed in section 5, the use of a LO generator and a specific implementation of the real photon emission in the final state does not bias the unfolded $A_{\mathrm{FB}}^{\mathrm{meas}}$ values. In order to assess the impact of these potential sources of systematic effects on the templates used to extract the $\sin^2\theta_{\mathrm{eff}}^{\mathrm{lept}}$ value, additional tests are performed. Effects related to the modelling of the real photon emission are tested with SHERPA, and are found to be negligible. The effects of NLO QCD corrections are investigated further in the context of the

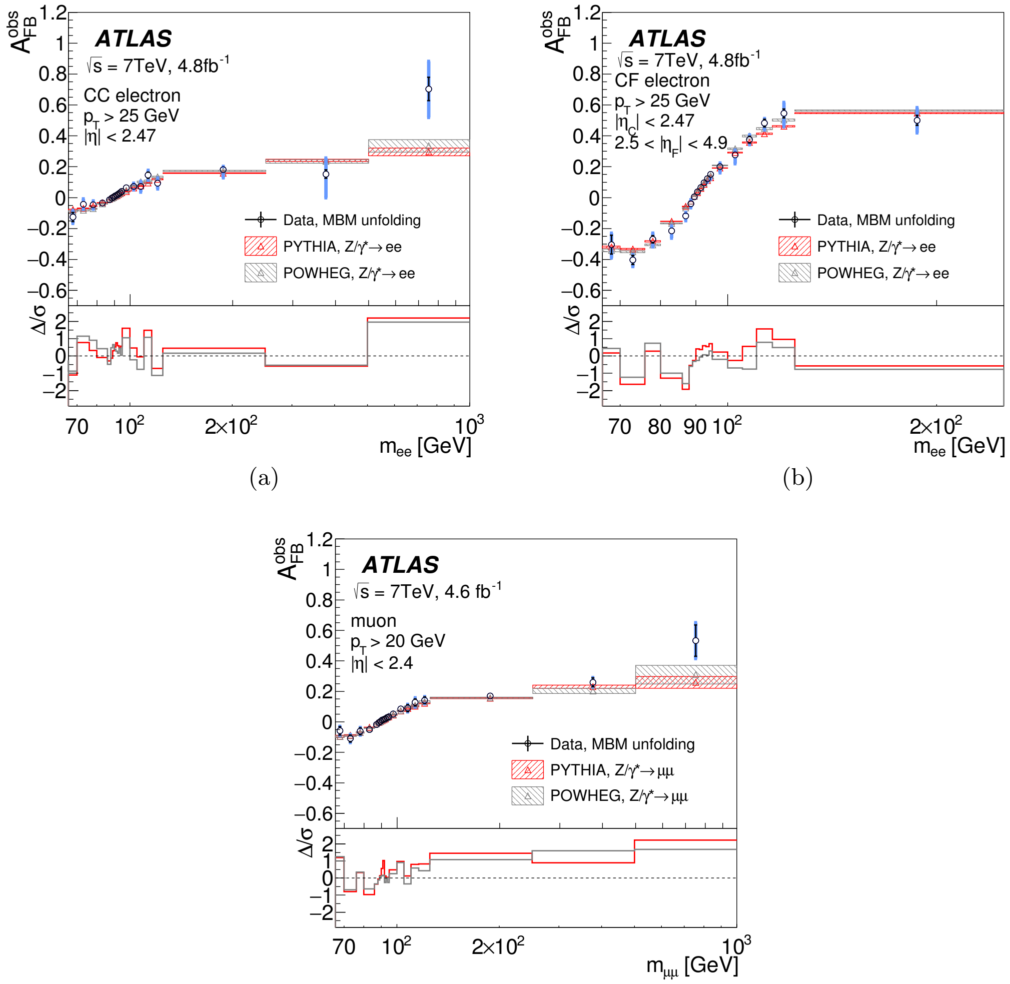

(a) (b) (c)

Figure 5. Forward-backward asymmetry ($A_{\rm FB}^{\rm obs}$) values as a function of the dilepton invariant mass for the (a) CC electron, (b) CF electron and (c) muon channels. Leptons are unfolded to Born level to account for mass bin migration, and the results are compared to truth-level MC information. For the data, the black inner error bars represent the statistical component and the lighter outer error bars the total error (statistical and systematic added in quadrature). The boxed shaded regions for the MC expectations represent only the statistical uncertainty; theoretical uncertainties are included in the systematic uncertainties on the data. The lower panel of each plot shows the pull values (Δ/σ, as defined for figure 3).

$\sin^2\theta_{\rm eff}^{\rm lept}$ measurement by comparing LO and NLO predictions of the $A_{\rm FB}$ vs. mass distributions calculated with MCFM [18]. Differences are propagated through the extraction of $\sin^2\theta_{\rm eff}^{\rm lept}$ and the resulting variation of the weak mixing angle is treated as an additional systematic error. The effects of NLO EWK corrections are found to be small compared to the rest of the uncertainties, but are accounted for as an additional systematic uncertainty on the final result.

The systematic uncertainties already described for the $A_{\rm FB}^{\rm meas}$ values are also estimated for the $\sin^2\theta_{\rm eff}^{\rm lept}$ measurement. As the background is small in all channels of the

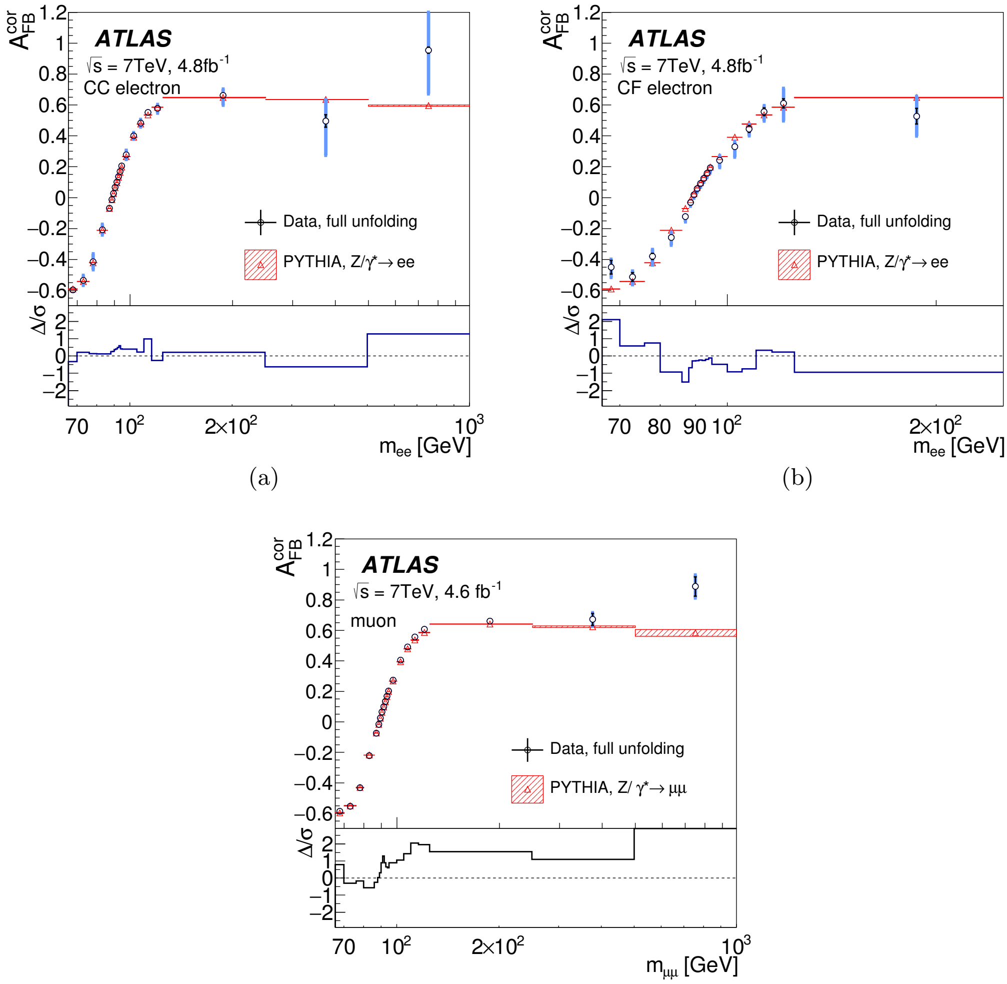

(a) (b) (c)

Figure 6. Forward-backward asymmetry ($A_{\rm FB}^{\rm cor}$) values as a function of the dilepton invariant mass for the (a) CC electron, (b) CF electron and (c) muon channels. Leptons are unfolded to Born level to account for mass bin migration and dilution effects are corrected. The measurement is extrapolated to the full phase space, and the results are compared to truth-level MC information. For the data, the black inner error bars represent the statistical component and the lighter outer error bars the total error (statistical and systematic added in quadrature). The boxed shaded regions for the MC expectations represent only the statistical uncertainty; theoretical uncertainties are included in the data systematic uncertainties. The lower panel of each plot shows the pull values (Δ/σ, as defined for figure 3).

$\sin^2\theta_{\rm eff}^{\rm lept}$ extraction, a simple, but slightly conservative, approach is used to obtain its uncertainty. The $\sin^2\theta_{\rm eff}^{\rm lept}$ measurement is repeated without the subtraction of the background, and the result is compared to the baseline measurement, which has the background subtracted. The uncertainty on $\sin^2\theta_{\rm eff}^{\rm lept}$ from the background is taken to be 10% of the observed difference, to take into account the uncertainties on the cross sections of the background components known with least precision [40].

6.1 Impact of PDFs on the $\sin^2\theta_{\rm eff}^{\rm lept}$ measurement

This measurement is sensitive to the PDFs describing the flavour composition of the initial state, since the $A_{\rm FB}$ values depend on the flavour and charge of the initial partons. In addition, the u_v and d_v valence quark distributions have an impact on the measurement due to differences in the weak couplings, while dilution effects introduce a dependence on the sea-to-valence quark ratio within the accessible Bjorken-x range.

The ATLAS measurements of inclusive W and Z boson production [41] are sensitive to the same effects and indicate that some of the existing PDF sets may not provide a good description of the data.

For this measurement of $\sin^2\theta_{\rm eff}^{\rm lept}$ a LO version of the ATLAS-epWZ NNLO and NLO fits was prepared. In the following, the PDFs extracted from these fits are called ATLAS-epWZ12 LO PDFs. These fits include inclusive W^+, W^- and Z production data at $\sqrt{s} = 7\,\text{TeV}$ [41], together with the combined HERA data on inclusive neutral- and charged-current interactions from e^+p and e^-p scattering [42]. The settings for the fit are kept the same as those for the NLO and NNLO fits as much as possible. The main differences between the LO fit and the higher-order fits are that the gluon PDF distribution has a simple parameterization which requires it to be positive definite at all scales, and that the value of the strong coupling constant $\alpha_{\rm s}(m_Z)$ is set to be higher than the one for the NLO or NNLO fits. A value of $\alpha_{\rm s}(m_Z)$ of 0.130 is chosen with a scanning procedure, such that it yields the best level of agreement (χ^2) between data and the fit result. This value is consistent with that used by other LO PDF sets. These PDFs are available in LHgrid formats [43].

6.2 Results for $\sin^2\theta_{\rm eff}^{\rm lept}$

The measured values of the weak mixing angle obtained with ATLAS-epWZ12 LO PDF are shown in table 2. Of the three channels, the CF electron channel has the lowest statistical uncertainty, despite having the fewest selected events, as detailed in section 4.3. This is because the $A_{\rm FB}^{\rm meas}$ values in this channel are less affected by dilution due to the larger average rapidity of the dilepton system compared to the other two channels. Details of the main sources of systematic uncertainty on the result in each channel are given in table 3.

The $\sin^2\theta_{\rm eff}^{\rm lept}$ measurements from all three channels are combined. Given the total covariance matrix C, the weights assigned to the three measurements for the combination are calculated using $w_i = \sum_k C^{-1}_{ik} / \sum_{jk} C^{-1}_{jk}$, with the indices i, j and k representing the three measurements (CC electron, CF electron, muon). The total error is given by $\sigma^2 = (W^{\rm T} C^{-1})^{-1} W$, with $W^{\rm T} = (1,1,1)$. Uncertainties due to energy/momentum scale and resolution are treated as completely uncorrelated across channels. Since the energy scale and resolution for the CF electron channel is dominated by the forward calorimeter performance, this is a good approximation for the correlation of the CC and CF electron channels. The systematic uncertainties due to the MC statistical uncertainty are also treated as fully uncorrelated. Theory-related systematic uncertainties, such as those associated with PDFs and higher-order EWK and QCD corrections, are treated as fully correlated across channels. All the remaining uncertainties are treated as fully correlated across the channels to which they are applicable. The central value of the combination is found to be stable when varying the magnitudes of the main correlated uncertainties. Following this procedure, the combined (CC+CF) electron result, as well as the electron-muon combination, is shown in table 2. The systematic uncertainty on the combined result is dominated by the PDF uncertainty (± 0.0009), which is calculated using the variations provided in the ATLAS-epWZ12 LO PDF eigenvalue set, similar to the calculation described in section 5. The contributions to the total systematic uncertainties on the results are included in table 3.

The results obtained with the ATLAS-epWZ12 LO PDF set have been compared to those obtained using other leading order PDF sets. The PDF sets ATLAS-epWZ12 LO and HERAPDF1.5LO [44] yield very similar results, the ATLAS-epWZ12 LO result being larger by 1×10^{-4} (with a PDF uncertainty of 9×10^{-4}). The MSTW2008LO set produces a downward shift in the resulting $\sin^2\theta_{\text{eff}}^{\text{lept}}$ which is significant ($\Delta\sin^2\theta_{\text{eff}}^{\text{lept}} = -2 \times 10^{-3}$). However, MSTW sets are known to give a poor description of the ATLAS W and Z data [41]. The CT10 PDF set (which is NLO) was also tested, and yields a $\sin^2\theta_{\text{eff}}^{\text{lept}}$ value which is smaller than, but compatible with, the results obtained with the ATLAS-epWZ12 LO PDF ($\Delta\sin^2\theta_{\text{eff}}^{\text{lept}} = -8 \times 10^{-4}$). The PDF analysis of the ATLAS data also suggests an increased strange-quark sea density ($\bar{s}/\bar{d} \sim 1$) compared to other PDF sets [15]. In order to probe the sensitivity of this measurement to the enhanced strange-quark density, a dedicated PDF set was prepared with a suppressed strange sea corresponding to uncertainty, which indicates a low sensitivity of the measurement to this effect. This is due to the fact that the sea composition only affects the measurement through the dilution, which, to first approximation, does not change the position of the minimum of the χ^2 in the template fits.

As a cross-check of the measured weak mixing angle and the unfolding procedure, $\sin^2\theta_{\text{eff}}^{\text{lept}}$ is extracted from the unfolded particle-level asymmetries. Similarly to the procedure described in the beginning of section 6, samples with various values of $\sin^2\theta_{\text{eff}}^{\text{lept}}$, generated using MCFM v6.8 [18] at LO in perturbative QCD and interfaced to APPLGRID v1.4.69 [45] using the ATLAS-epWZ12 LO PDF set, are compared to the measured particle-level asymmetries using a χ^2 test. The correlations between the systematic uncertainties are included in the χ^2 calculation. A parabolic fit to the χ^2 distribution yields a value of $\sin^2\theta_{\text{eff}}^{\text{lept}}$ in good agreement with the detector-level extraction.

There are several other measurements of $\sin^2\theta_{\text{eff}}^{\text{lept}}$ at the m_Z scale. The results from this analysis, as well as the results from the other collider experiments, are summarized in table 4 and shown in figure 7. These include measurements from LEP, SLC, the Tevatron, and the LHC, as well as the results of the PDG global fit [46]. Differences with respect to the combined LEP/SLC measurements are also displayed. The combined result of this analysis agrees within $0.1\,\sigma$ with the most precise leptonic asymmetry measurement, and within $1.2\,\sigma$ of the $\sin^2\theta_{\text{eff}}^{\text{lept}}$ value extracted from the LEP $A_{\text{FB}}^{0,b}$ measurement. The combined result is in agreement with the PDG global fit at the level of $0.6\,\sigma$.

6.3 Determination of A_μ

As described in section 1, the forward-backward asymmetry around the Z pole for the muon channel, $A_{\text{FB}}^{0,\mu}$, can be expressed in terms of the muon and quark asymmetry parameters A_μ

	$\sin^2\theta_{\mathrm{eff}}^{\mathrm{lept}}$
CC electron	$0.2302 \pm 0.0009(\mathrm{stat.}) \pm 0.0008(\mathrm{syst.}) \pm 0.0010(\mathrm{PDF}) = 0.2302 \pm 0.0016$
CF electron	$0.2312 \pm 0.0007(\mathrm{stat.}) \pm 0.0008(\mathrm{syst.}) \pm 0.0010(\mathrm{PDF}) = 0.2312 \pm 0.0014$
Muon	$0.2307 \pm 0.0009(\mathrm{stat.}) \pm 0.0008(\mathrm{syst.}) \pm 0.0009(\mathrm{PDF}) = 0.2307 \pm 0.0015$
El. combined	$0.2308 \pm 0.0006(\mathrm{stat.}) \pm 0.0007(\mathrm{syst.}) \pm 0.0010(\mathrm{PDF}) = 0.2308 \pm 0.0013$
Combined	$0.2308 \pm 0.0005(\mathrm{stat.}) \pm 0.0006(\mathrm{syst.}) \pm 0.0009(\mathrm{PDF}) = 0.2308 \pm 0.0012$

Table 2. The $\sin^2\theta_{\mathrm{eff}}^{\mathrm{lept}}$ measurement results in each of the three studied channels: electron central-central, electron central-forward and muon. Results of the statistical combination of both electron channels and all three channels are shown as well.

Uncertainty source	CC electrons $[10^{-4}]$	CF electrons $[10^{-4}]$	Muons $[10^{-4}]$	Combined $[10^{-4}]$
PDF	10	10	9	9
MC statistics	5	2	5	2
Electron energy scale	4	6	—	3
Electron energy resolution	4	5	—	2
Muon energy scale	—	—	5	2
Higher-order corrections	3	1	3	2
Other sources	1	1	2	2

Table 3. Contributions to the systematic uncertainties on the $\sin^2\theta_{\mathrm{eff}}^{\mathrm{lept}}$ values extracted from the three analysis channels and on the combined result. Null entries (denoted by "—") correspond to uncertainties that do not apply to a specific channel. Higher-order corrections include NLO QCD and NLO EWK contributions. Other sources include the effect of pileup, background uncertainties, lepton trigger/reconstruction/identification efficiency uncertainties, muon momentum resolution and effects of detector misalignment.

and A_q, cf. eq. 1.4 and ref. [3]. Both are functions of the vector and axial-vector couplings of the quark/muon,

$$A_{q/\mu} = \frac{2g_{\mathrm{V}}^{q/\mu} g_{\mathrm{A}}^{q/\mu}}{(g_{\mathrm{V}}^{q/\mu})^2 + (g_{\mathrm{A}}^{q/\mu})^2} = \frac{2g_{\mathrm{V}}^{q/\mu}/g_{\mathrm{A}}^{q/\mu}}{1 + (g_{\mathrm{V}}^{q/\mu}/g_{\mathrm{A}}^{q/\mu})^2}. \tag{6.1}$$

The asymmetry parameters are related to the flavour-dependent weak mixing angle $\sin^2\theta_{\mathrm{eff}}^{q/\mu}$ by

$$g_{\mathrm{V}}^{q/\mu}/g_{\mathrm{A}}^{q/\mu} = 1 - 4|Q_{q/\mu}|\sin^2\theta_{\mathrm{eff}}^{q/\mu}, \tag{6.2}$$

where $Q_{q/\mu}$ is the quark (q) or muon (μ) charge. The measurement of the forward-backward asymmetry can be interpreted as a determination of A_μ when assuming $\sin^2\theta_{\mathrm{eff}}^{q} = \sin^2\theta_{\mathrm{eff}}^{\mu} = \sin^2\theta_{\mathrm{eff}}^{\mathrm{lept}}$, which is valid within an uncertainty of 1.5×10^{-4} [3]. Given the value of

JHEP09(2015)049

	$\sin^2\theta_{\rm eff}^{\rm lept}$	Δ/σ (w.r.t. LEP+SLC)	Δ/σ (w.r.t. ATLAS)
CMS [6]	0.2287 ± 0.0032	-0.9	-0.6
D0 [5]	0.23146 ± 0.00047	-0.1	0.5
CDF [4]	0.2315 ± 0.0010	-0.03	0.4
LEP, $A_{\rm FB}^{0,b}$ [3]	0.23221 ± 0.00029	—	1.2
LEP, $A_{\rm FB}^{0,l}$ [3]	0.23099 ± 0.00053	—	-0.1
SLC, $A_{\rm LR}$ [3]	0.23098 ± 0.00026	—	-0.1
LEP+SLC [3]	0.23153 ± 0.00016	—	0.6
PDG global fit [46]	0.23146 ± 0.00012	-0.4	0.6
ATLAS	0.2308 ± 0.0012	-0.6	—

Table 4. Comparison of the results of this analysis with other published results for $\sin^2\theta_{\rm eff}^{\rm lept}$. The comparison includes the most precise measurements from LEP and SLC, and the results from the leptonic $\sin^2\theta_{\rm eff}^{\rm lept}$ measurements from the hadron collider experiments CMS, D0, and CDF. Also shown are the values of $\sin^2\theta_{\rm eff}^{\rm lept}$ from the LEP+SLC global combination (which includes all $\sin^2\theta_{\rm eff}^{\rm lept}$ measurements performed at the two colliders) and from the PDG global fit. Each Δ/σ column shows the difference between the result and the quoted reference value, divided by the quadratic sum of the associated uncertainties.

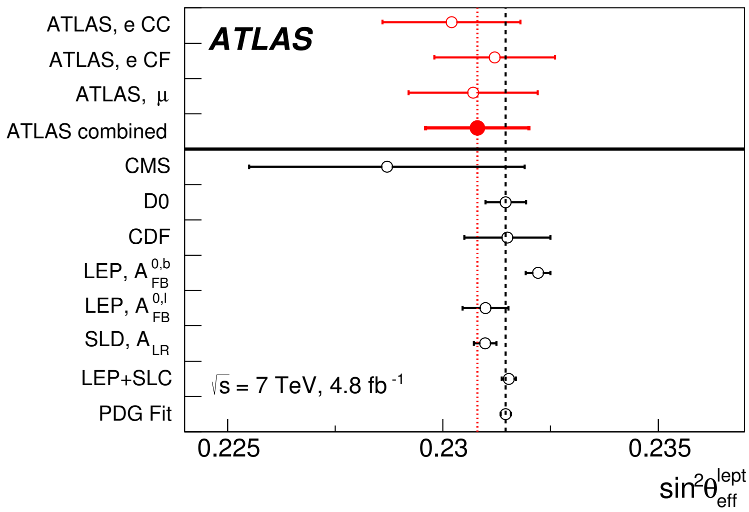

Figure 7. Comparison of the results of this analysis with other published results for $\sin^2\theta_{\rm eff}^{\rm lept}$. This includes the most precise measurements from LEP and SLC, and the leptonic $\sin^2\theta_{\rm eff}^{\rm lept}$ measurements from the hadron collider experiments CMS [6], D0 [5], and CDF [4]. Also shown are the values of $\sin^2\theta_{\rm eff}^{\rm lept}$ from the LEP+SLC global combination [3] (which includes all $\sin^2\theta_{\rm eff}^{\rm lept}$ measurements performed at the two colliders) and from the PDG global fit [46]. The vertical dotted line shows the central value of the ATLAS combined measurement reported here, while the vertical dashed line represents that of the current PDG global fit [46].

JHEP09(2015)049

$\sin^2\theta_{\text{eff}}^{\text{lept}}$, A_μ is small compared to A_q and the uncertainty on $\sin^2\theta_{\text{eff}}^{\mu}$ ($\sim 1.5\times 10^{-3}$) plays a more important role in eq. 1.4 than the error introduced by the assumption about $\sin^2\theta_{\text{eff}}^{q}$ mentioned above. With the present precision, it is therefore possible to use the value of $\sin^2\theta_{\text{eff}}^{\mu}$ obtained from the muon asymmetry measurement to derive

$$A_\mu = \frac{2(1-4\sin^2\theta_{\text{eff}}^{\text{lept}})}{1+(1-4\sin^2\theta_{\text{eff}}^{\text{lept}})^2}. \tag{6.3}$$

The uncertainties on A_μ are propagated from the uncertainties on $\sin^2\theta_{\text{eff}}^{\text{lept}}$. The result is

$$A_\mu = 0.153 \pm 0.007(\text{stat.}) \pm 0.006(\text{syst.}) \pm 0.007(\text{PDF}) = 0.153 \pm 0.012(\text{tot.}),$$

which is of similar precision and in good agreement with the measurement from e^+e^- collisions of 0.142 ± 0.015 [3]. It is worth stressing, however, that the determination of A_μ in the LEP/SLD results is based entirely on asymmetry measurements in the different lepton final states without any assumptions on other A_f, whereas the determination of A_μ presented here uses the Standard Model prediction of A_q.

7 Conclusions

The forward-backward asymmetry in electron and muon pairs from Z/γ^* decays is measured using the 7 TeV pp LHC collision data recorded with the ATLAS detector in 2011 corresponding to an integrated luminosity of 4.8 fb^{-1}. The data are analysed over a range of dilepton invariant masses from 66 GeV to 1000 GeV in the central-central electron and muon channels, and up to 250 GeV in the central-forward electron channel. The latter includes events where one electron is reconstructed in the forward pseudorapidity range ($2.5 < |\eta| < 4.9$).

The forward-backward asymmetry is measured separately for the three channels as a function of the dilepton invariant mass and unfolded for detector effects and final-state radiation. Additionally, a leading-order interpretation which accounts for the effects of dilution and full detector acceptance is presented. The resulting A_{FB} values are found to be in agreement with the corresponding Standard Model predictions.

The detector level asymmetry values are used to extract the value of the leptonic effective weak mixing angle, $\sin^2\theta_{\text{eff}}^{\text{lept}}$, separately for the three data samples using a χ^2 minimization method. The results are in good agreement with each other and with measurements at e^+e^- colliders, at the Tevatron and by CMS at the LHC.

Results from the electron and muon final states are combined, yielding

$$\sin^2\theta_{\text{eff}}^{\text{lept}} = 0.2308 \pm 0.0005(\text{stat.}) \pm 0.0006(\text{syst.}) \pm 0.0009(\text{PDF}) = 0.2308 \pm 0.0012(\text{tot.}).$$

The dominant uncertainty comes from knowledge of the PDFs.

The result from the muon channel, when converted to the asymmetry parameter A_μ, yields

$$A_\mu = 0.153 \pm 0.007(\text{stat.}) \pm 0.006(\text{syst.}) \pm 0.007(\text{PDF}) = 0.153 \pm 0.012(\text{tot.}),$$

which is in good agreement with the best previous measurements.

JHEP09(2015)049

Acknowledgments

We thank CERN for the very successful operation of the LHC, as well as the support staff from our institutions without whom ATLAS could not be operated efficiently.

We acknowledge the support of ANPCyT, Argentina; YerPhI, Armenia; ARC, Australia; BMWFW and FWF, Austria; ANAS, Azerbaijan; SSTC, Belarus; CNPq and FAPESP, Brazil; NSERC, NRC and CFI, Canada; CERN; CONICYT, Chile; CAS, MOST and NSFC, China; COLCIENCIAS, Colombia; MSMT CR, MPO CR and VSC CR, Czech Republic; DNRF, DNSRC and Lundbeck Foundation, Denmark; EPLANET, ERC and NSRF, European Union; IN2P3-CNRS, CEA-DSM/IRFU, France; GNSF, Georgia; BMBF, DFG, HGF, MPG and AvH Foundation, Germany; GSRT and NSRF, Greece; RGC, Hong Kong SAR, China; ISF, MINERVA, GIF, I-CORE and Benoziyo Center, Israel; INFN, Italy; MEXT and JSPS, Japan; CNRST, Morocco; FOM and NWO, Netherlands; BRF and RCN, Norway; MNiSW and NCN, Poland; GRICES and FCT, Portugal; MNE/IFA, Romania; MES of Russia and NRC KI, Russian Federation; JINR; MSTD, Serbia; MSSR, Slovakia; ARRS and MIZŠ, Slovenia; DST/NRF, South Africa; MINECO, Spain; SRC and Wallenberg Foundation, Sweden; SER, SNSF and Cantons of Bern and Geneva, Switzerland; NSC, Taiwan; TAEK, Turkey; STFC, the Royal Society and Leverhulme Trust, United Kingdom; DOE and NSF, United States of America.

The crucial computing support from all WLCG partners is acknowledged gratefully, in particular from CERN and the ATLAS Tier-1 facilities at TRIUMF (Canada), NDGF (Denmark, Norway, Sweden), CC-IN2P3 (France), KIT/GridKA (Germany), INFN-CNAF (Italy), NL-T1 (Netherlands), PIC (Spain), ASGC (Taiwan), RAL (U.K.) and BNL (U.S.A.) and in the Tier-2 facilities worldwide.

References

[1] J.C. Collins and D.E. Soper, *Angular distribution of dileptons in high-energy hadron collisions*, *Phys. Rev.* **D 16** (1977) 2219 [INSPIRE].

[2] A. Sirlin, *Radiative corrections in the* $\mathrm{SU}(2)_L \times \mathrm{U}(1)$ *theory: a simple renormalization framework*, *Phys. Rev.* **D 22** (1980) 971 [INSPIRE].

[3] SLD Electroweak Group, DELPHI, ALEPH, SLD, SLD Heavy Flavour Group, OPAL, LEP Electroweak Working Group, L3 collaboration, S. Schael et al., *Precision electroweak measurements on the Z resonance*, *Phys. Rept.* **427** (2006) 257 [hep-ex/0509008] [INSPIRE].

[4] CDF collaboration, T.A. Aaltonen et al., *Indirect measurement of* $\sin^2\theta_W$ *(or* M_W*) using* $\mu^+\mu^-$ *pairs from* γ^*/Z *bosons produced in* $p\bar{p}$ *collisions at a center-of-momentum energy of* 1.96 *TeV*, *Phys. Rev.* **D 89** (2014) 072005 [arXiv:1402.2239] [INSPIRE].

[5] D0 collaboration, V.M. Abazov et al., *Measurement of the effective weak mixing angle in $p\bar{p} \to Z/\gamma^* \to e^+e^-$ events*, *Phys. Rev. Lett.* **115** (2015) 041801 [arXiv:1408.5016] [INSPIRE].

[6] CMS collaboration, *Measurement of the weak mixing angle with the Drell-Yan process in proton-proton collisions at the LHC*, *Phys. Rev.* **D 84** (2011) 112002 [arXiv:1110.2682] [INSPIRE].

[7] CMS collaboration, *Forward-backward asymmetry of Drell-Yan lepton pairs in pp collisions at $\sqrt{s} = 7$ TeV*, *Phys. Lett.* **B 718** (2013) 752 [arXiv:1207.3973] [INSPIRE].

[8] ATLAS collaboration, *The ATLAS experiment at the CERN Large Hadron Collider*, 2008 *JINST* **3** S08003 [INSPIRE].

[9] L. Evans and P. Bryant, *LHC machine*, 2008 *JINST* **3** S08001 [INSPIRE].

[10] ATLAS collaboration, *The ATLAS simulation infrastructure*, *Eur. Phys. J.* **C 70** (2010) 823 [arXiv:1005.4568] [INSPIRE].

[11] GEANT4 collaboration, S. Agostinelli et al., *GEANT4: a simulation toolkit*, *Nucl. Instrum. Meth.* **A 506** (2003) 250 [INSPIRE].

[12] T. Sjöstrand, S. Mrenna and P.Z. Skands, *PYTHIA 6.4 physics and manual*, *JHEP* **05** (2006) 026 [hep-ph/0603175] [INSPIRE].

[13] A.D. Martin, W.J. Stirling, R.S. Thorne and G. Watt, *Parton distributions for the LHC*, *Eur. Phys. J.* **C 63** (2009) 189 [arXiv:0901.0002] [INSPIRE].

[14] P. Golonka and Z. Was, *PHOTOS Monte Carlo: a precision tool for QED corrections in Z and W decays*, *Eur. Phys. J.* **C 45** (2006) 97 [hep-ph/0506026] [INSPIRE].

[15] ATLAS collaboration, *Determination of the strange quark density of the proton from ATLAS measurements of the $W \to \ell\nu$ and $Z \to \ell\ell$ cross sections*, *Phys. Rev. Lett.* **109** (2012) 012001 [arXiv:1203.4051] [INSPIRE].

[16] R. Hamberg, W.L. van Neerven and T. Matsuura, *A complete calculation of the order α_s^2 correction to the Drell-Yan K factor*, *Nucl. Phys.* **B 359** (1991) 343 [*Erratum ibid.* **B 644** (2002) 403] [INSPIRE].

[17] C.M. Carloni Calame, G. Montagna, O. Nicrosini and A. Vicini, *Precision electroweak calculation of the production of a high transverse-momentum lepton pair at hadron colliders*, *JHEP* **10** (2007) 109 [arXiv:0710.1722] [INSPIRE].

[18] J.M. Campbell and R.K. Ellis, *MCFM for the Tevatron and the LHC*, *Nucl. Phys. Proc. Suppl.* **205-206** (2010) 10 [arXiv:1007.3492] [INSPIRE].

[19] S. Alioli, P. Nason, C. Oleari and E. Re, *NLO vector-boson production matched with shower in POWHEG*, *JHEP* **07** (2008) 060 [arXiv:0805.4802] [INSPIRE].

[20] G. Corcella et al., *HERWIG 6: an event generator for hadron emission reactions with interfering gluons (including supersymmetric processes)*, *JHEP* **01** (2001) 010 [hep-ph/0011363] [INSPIRE].

[21] G. Corcella, I.G. Knowles, G. Marchesini, S. Moretti, K. Odagiri, P. Richardson et al., *HERWIG 6: an event generator for hadron emission reactions with interfering gluons (including supersymmetric processes)*, *JHEP* **01** (2001) 010 [hep-ph/0011363] [INSPIRE].

[22] A. Sherstnev and R. Thorne, *Different PDF approximations useful for LO Monte Carlo generators*, arXiv:0807.2132.

[23] S. Frixione and B.R. Webber, *Matching NLO QCD computations and parton shower simulations*, *JHEP* **06** (2002) 029 [hep-ph/0204244] [INSPIRE].

[24] S. Frixione, P. Nason and B.R. Webber, *Matching NLO QCD and parton showers in heavy flavor production*, *JHEP* **08** (2003) 007 [hep-ph/0305252] [INSPIRE].

[25] J. Pumplin, D.R. Stump, J. Huston, H.L. Lai, P.M. Nadolsky and W.K. Tung, *New generation of parton distributions with uncertainties from global QCD analysis*, *JHEP* **07** (2002) 012 [hep-ph/0201195] [INSPIRE].

[26] ATLAS collaboration, *Electron performance measurements with the ATLAS detector using the 2010 LHC proton-proton collision data*, *Eur. Phys. J.* **C 72** (2012) 1909 [arXiv:1110.3174] [INSPIRE].

[27] ATLAS collaboration, *Electron reconstruction and identification efficiency measurements with the ATLAS detector using the 2011 LHC proton-proton collision data*, *Eur. Phys. J.* **C 74** (2014) 2941 [arXiv:1404.2240] [INSPIRE].

[28] ATLAS collaboration, *Muon reconstruction efficiency and momentum resolution of the ATLAS experiment in proton-proton collisions at $\sqrt{s} = 7$ TeV in 2010*, *Eur. Phys. J.* **C 74** (2014) 3034 [arXiv:1404.4562] [INSPIRE].

[29] ATLAS collaboration, *Measurement of the muon reconstruction performance of the ATLAS detector using 2011 and 2012 LHC proton-proton collision data*, *Eur. Phys. J.* **C 74** (2014) 3130 [arXiv:1407.3935] [INSPIRE].

[30] ATLAS collaboration, *Measurement of the $W \to \ell\nu$ and $Z/\gamma^* \to \ell\ell$ production cross sections in proton-proton collisions at $\sqrt{s} = 7$ TeV with the ATLAS detector*, *JHEP* **12** (2010) 060 [arXiv:1010.2130] [INSPIRE].

[31] ATLAS collaboration, *Search for high-mass dilepton resonances in pp collisions at $\sqrt{s} = 8$ TeV with the ATLAS detector*, *Phys. Rev.* **D 90** (2014) 052005 [arXiv:1405.4123] [INSPIRE].

[32] The Durham HepData project, http://hepdata.cedar.ac.uk/.

[33] U. Baur, S. Keller and W.K. Sakumoto, *QED radiative corrections to Z boson production and the forward backward asymmetry at hadron colliders*, *Phys. Rev.* **D 57** (1998) 199 [hep-ph/9707301] [INSPIRE].

[34] G. D'Agostini, *A multidimensional unfolding method based on Bayes' theorem*, *Nucl. Instrum. Meth.* **A 362** (1995) 487 [INSPIRE].

[35] T. Adye, *Unfolding algorithms and tests using RooUnfold*, arXiv:1105.1160.

[36] T. Gleisberg et al., *Event generation with SHERPA 1.1*, *JHEP* **02** (2009) 007 [arXiv:0811.4622] [INSPIRE].

[37] M. Schonherr and F. Krauss, *Soft photon radiation in particle decays in SHERPA*, *JHEP* **12** (2008) 018 [arXiv:0810.5071] [INSPIRE].

[38] ATLAS collaboration, *Study of alignment-related systematic effects on the ATLAS Inner Detector tracking*, ATLAS-CONF-2012-141 (2012).

[39] H.-L. Lai et al., *New parton distributions for collider physics*, *Phys. Rev.* **D 82** (2010) 074024 [arXiv:1007.2241] [INSPIRE].

[40] ATLAS collaboration, *Measurement of ZZ production in pp collisions at $\sqrt{s} = 7$ TeV and limits on anomalous ZZZ and ZZγ couplings with the ATLAS detector*, *JHEP* **03** (2013) 128 [arXiv:1211.6096] [INSPIRE].

JHEP09(2015)049

[41] ATLAS collaboration, *Measurement of the inclusive $W^{\pm}$ and Z/γ cross sections in the electron and muon decay channels in pp collisions at $\sqrt{s} = 7$ TeV with the ATLAS detector*, *Phys. Rev.* **D 85** (2012) 072004 [arXiv:1109.5141] [INSPIRE].

[42] ZEUS, H1 collaboration, F.D. Aaron et al., *Combined measurement and QCD analysis of the inclusive $e^{\pm}p$ scattering cross sections at HERA*, *JHEP* **01** (2010) 109 [arXiv:0911.0884] [INSPIRE].

[43] M. Whalley, D. Bourilkov and R. Group, *The Les Houches accord PDFs (LHAPDF) and LHAGLUE*, hep-ph/0508110.

[44] H1 and ZEUS collaborations, *HERAPDF1.5LO PDF set with experimental uncertainties*, H1PRELIM-13-141 (2013) [ZEUS-PREL-13-003].

[45] T. Carli et al., *A posteriori inclusion of parton density functions in NLO QCD final-state calculations at hadron colliders: the APPLGRID project*, *Eur. Phys. J.* **C 66** (2010) 503 [arXiv:0911.2985] [INSPIRE].

[46] Particle Data Group collaboration, K. Nakamura et al., *Review of particle physics*, *J. Phys.* **G 37** (2010) 075021 [INSPIRE].

JHEP09(2015)049

The ATLAS collaboration

G. Aad[84], B. Abbott[112], J. Abdallah[152], S. Abdel Khalek[116], O. Abdinov[11], R. Aben[106], B. Abi[113], M. Abolins[89], O.S. AbouZeid[159], H. Abramowicz[154], H. Abreu[153], R. Abreu[30], Y. Abulaiti[147a,147b], B.S. Acharya[165a,165b,a], L. Adamczyk[38a], D.L. Adams[25], J. Adelman[177], S. Adomeit[99], T. Adye[130], T. Agatonovic-Jovin[13a], J.A. Aguilar-Saavedra[125a,125f], M. Agustoni[17], S.P. Ahlen[22], F. Ahmadov[64,b], G. Aielli[134a,134b], H. Akerstedt[147a,147b], T.P.A. Åkesson[80], G. Akimoto[156], A.V. Akimov[95], G.L. Alberghi[20a,20b], J. Albert[170], S. Albrand[55], M.J. Alconada Verzini[70], M. Aleksa[30], I.N. Aleksandrov[64], C. Alexa[26a], G. Alexander[154], G. Alexandre[49], T. Alexopoulos[10], M. Alhroob[165a,165c], G. Alimonti[90a], L. Alio[84], J. Alison[31], B.M.M. Allbrooke[18], L.J. Allison[71], P.P. Allport[73], J. Almond[83], A. Aloisio[103a,103b], A. Alonso[36], F. Alonso[70], C. Alpigiani[75], A. Altheimer[35], B. Alvarez Gonzalez[89], M.G. Alviggi[103a,103b], K. Amako[65], Y. Amaral Coutinho[24a], C. Amelung[23], D. Amidei[88], S.P. Amor Dos Santos[125a,125c], A. Amorim[125a,125b], S. Amoroso[48], N. Amram[154], G. Amundsen[23], C. Anastopoulos[140], L.S. Ancu[49], N. Andari[30], T. Andeen[35], C.F. Anders[58b], G. Anders[30], K.J. Anderson[31], A. Andreazza[90a,90b], V. Andrei[58a], X.S. Anduaga[70], S. Angelidakis[9], I. Angelozzi[106], P. Anger[44], A. Angerami[35], F. Anghinolfi[30], A.V. Anisenkov[108,c], N. Anjos[125a], A. Annovi[47], A. Antonaki[9], M. Antonelli[47], A. Antonov[97], J. Antos[145b], F. Anulli[133a], M. Aoki[65], L. Aperio Bella[18], R. Apolle[119,d], G. Arabidze[89], I. Aracena[144], Y. Arai[65], J.P. Araque[125a], A.T.H. Arce[45], J-F. Arguin[94], S. Argyropoulos[42], M. Arik[19a], A.J. Armbruster[30], O. Arnaez[30], V. Arnal[81], H. Arnold[48], M. Arratia[28], O. Arslan[21], A. Artamonov[96], G. Artoni[23], S. Asai[156], N. Asbah[42], A. Ashkenazi[154], B. Åsman[147a,147b], L. Asquith[6], K. Assamagan[25], R. Astalos[145a], M. Atkinson[166], N.B. Atlay[142], B. Auerbach[6], K. Augsten[127], M. Aurousseau[146b], G. Avolio[30], G. Azuelos[94,e], Y. Azuma[156], M.A. Baak[30], C. Bacci[135a,135b], H. Bachacou[137], K. Bachas[155], M. Backes[30], M. Backhaus[30], J. Backus Mayes[144], E. Badescu[26a], P. Bagiacchi[133a,133b], P. Bagnaia[133a,133b], Y. Bai[33a], T. Bain[35], J.T. Baines[130], O.K. Baker[177], S. Baker[77], P. Balek[128], F. Balli[137], E. Banas[39], Sw. Banerjee[174], A.A.E. Bannoura[176], V. Bansal[170], H.S. Bansil[18], L. Barak[173], S.P. Baranov[95], E.L. Barberio[87], D. Barberis[50a,50b], M. Barbero[84], T. Barillari[100], M. Barisonzi[176], T. Barklow[144], N. Barlow[28], B.M. Barnett[130], R.M. Barnett[15], Z. Barnovska[5], A. Baroncelli[135a], G. Barone[49], A.J. Barr[119], F. Barreiro[81], J. Barreiro Guimarães da Costa[57], R. Bartoldus[144], A.E. Barton[71], P. Bartos[145a], V. Bartsch[150], A. Bassalat[116], A. Basye[166], R.L. Bates[53], L. Batkova[145a], J.R. Batley[28], M. Battaglia[138], M. Battistin[30], F. Bauer[137], H.S. Bawa[144,f], T. Beau[79], P.H. Beauchemin[162], R. Beccherle[123a,123b], P. Bechtle[21], H.P. Beck[17,g], K. Becker[176], S. Becker[99], M. Beckingham[139], C. Becot[116], A.J. Beddall[19c], A. Beddall[19c], S. Bedikian[177], V.A. Bednyakov[64], C.P. Bee[149], L.J. Beemster[106], T.A. Beermann[176], M. Begel[25], K. Behr[119], C. Belanger-Champagne[86], P.J. Bell[49], W.H. Bell[49], G. Bella[154], L. Bellagamba[20a], A. Bellerive[29], M. Bellomo[85], K. Belotskiy[97], O. Beltramello[30], O. Benary[154], D. Benchekroun[136a], K. Bendtz[147a,147b], N. Benekos[166], Y. Benhammou[154], E. Benhar Noccioli[49], J.A. Benitez Garcia[160b], D.P. Benjamin[45], J.R. Bensinger[23], K. Benslama[131], S. Bentvelsen[106], D. Berge[106], E. Bergeaas Kuutmann[16], N. Berger[5], F. Berghaus[170], E. Berglund[106], J. Beringer[15], C. Bernard[22], P. Bernat[77], C. Bernius[78], F.U. Bernlochner[170], T. Berry[76], P. Berta[128], C. Bertella[84], G. Bertoli[147a,147b], F. Bertolucci[123a,123b], D. Bertsche[112], M.I. Besana[90a], G.J. Besjes[105], O. Bessidskaia Bylund[147a,147b], M. Bessner[42], N. Besson[137], C. Betancourt[48], S. Bethke[100], W. Bhimji[46], R.M. Bianchi[124], L. Bianchini[23], M. Bianco[30], O. Biebel[99], S.P. Bieniek[77], K. Bierwagen[54], J. Biesiada[15], M. Biglietti[135a], J. Bilbao De Mendizabal[49], H. Bilokon[47], M. Bindi[54], S. Binet[116], A. Bingul[19c], C. Bini[133a,133b], C.W. Black[151], J.E. Black[144], K.M. Black[22], D. Blackburn[139], R.E. Blair[6], J.-B. Blanchard[137], T. Blazek[145a], I. Bloch[42], C. Blocker[23], W. Blum[82,*], U. Blumenschein[54], G.J. Bobbink[106], V.S. Bobrovnikov[108,c], S.S. Bocchetta[80], A. Bocci[45],

JHEP09(2015)049

C. Bock[99], C.R. Boddy[119], M. Boehler[48], J. Boek[176], T.T. Boek[176], J.A. Bogaerts[30], A.G. Bogdanchikov[108], A. Bogouch[91,*], C. Bohm[147a], J. Bohm[126], V. Boisvert[76], T. Bold[38a], V. Boldea[26a], A.S. Boldyrev[98], M. Bomben[79], M. Bona[75], M. Boonekamp[137], A. Borisov[129], G. Borissov[71], M. Borri[83], S. Borroni[42], J. Bortfeldt[99], V. Bortolotto[135a,135b], K. Bos[106], D. Boscherini[20a], M. Bosman[12], H. Boterenbrood[106], J. Boudreau[124], J. Bouffard[2], E.V. Bouhova-Thacker[71], D. Boumediene[34], C. Bourdarios[116], N. Bousson[113], S. Boutouil[136d], A. Boveia[31], J. Boyd[30], I.R. Boyko[64], I. Bozovic-Jelisavcic[13b], J. Bracinik[18], A. Brandt[8], G. Brandt[15], O. Brandt[58a], U. Bratzler[157], B. Brau[85], J.E. Brau[115], H.M. Braun[176,*], S.F. Brazzale[165a,165c], B. Brelier[159], K. Brendlinger[121], A.J. Brennan[87], R. Brenner[167], S. Bressler[173], K. Bristow[146c], T.M. Bristow[46], D. Britton[53], F.M. Brochu[28], I. Brock[21], R. Brock[89], C. Bromberg[89], J. Bronner[100], G. Brooijmans[35], T. Brooks[76], W.K. Brooks[32b], J. Brosamer[15], E. Brost[115], G. Brown[83], J. Brown[55], P.A. Bruckman de Renstrom[39], D. Bruncko[145b], R. Bruneliere[48], S. Brunet[60], A. Bruni[20a], G. Bruni[20a], M. Bruschi[20a], L. Bryngemark[80], T. Buanes[14], Q. Buat[143], F. Bucci[49], P. Buchholz[142], R.M. Buckingham[119], A.G. Buckley[53], S.I. Buda[26a], I.A. Budagov[64], F. Buehrer[48], L. Bugge[118], M.K. Bugge[118], O. Bulekov[97], A.C. Bundock[73], H. Burckhart[30], S. Burdin[73], B. Burghgrave[107], S. Burke[130], I. Burmeister[43], E. Busato[34], D. Büscher[48], V. Büscher[82], P. Bussey[53], C.P. Buszello[167], B. Butler[57], J.M. Butler[22], A.I. Butt[3], C.M. Buttar[53], J.M. Butterworth[77], P. Butti[106], W. Buttinger[28], A. Buzatu[53], M. Byszewski[10], S. Cabrera Urbán[168], D. Caforio[20a,20b], O. Cakir[4a], P. Calafiura[15], A. Calandri[137], G. Calderini[79], P. Calfayan[99], R. Calkins[107], L.P. Caloba[24a], D. Calvet[34], S. Calvet[34], R. Camacho Toro[49], S. Camarda[42], D. Cameron[118], L.M. Caminada[15], R. Caminal Armadans[12], S. Campana[30], M. Campanelli[77], A. Campoverde[149], V. Canale[103a,103b], A. Canepa[160a], M. Cano Bret[75], J. Cantero[81], R. Cantrill[76], T. Cao[40], M.D.M. Capeans Garrido[30], I. Caprini[26a], M. Caprini[26a], M. Capua[37a,37b], R. Caputo[82], R. Cardarelli[134a], T. Carli[30], G. Carlino[103a], L. Carminati[90a,90b], S. Caron[105], E. Carquin[32a], G.D. Carrillo-Montoya[146c], J.R. Carter[28], J. Carvalho[125a,125c], D. Casadei[77], M.P. Casado[12], M. Casolino[12], E. Castaneda-Miranda[146b], A. Castelli[106], V. Castillo Gimenez[168], N.F. Castro[125a], P. Catastini[57], A. Catinaccio[30], J.R. Catmore[118], A. Cattai[30], G. Cattani[134a,134b], S. Caughron[89], V. Cavaliere[166], D. Cavalli[90a], M. Cavalli-Sforza[12], V. Cavasinni[123a,123b], F. Ceradini[135a,135b], B.C. Cerio[45], K. Cerny[128], A.S. Cerqueira[24b], A. Cerri[150], L. Cerrito[75], F. Cerutti[15], M. Cerv[30], A. Cervelli[17], S.A. Cetin[19b], A. Chafaq[136a], D. Chakraborty[107], I. Chalupkova[128], K. Chan[3], P. Chang[166], B. Chapleau[86], J.D. Chapman[28], D. Charfeddine[116], D.G. Charlton[18], C.C. Chau[159], C.A. Chavez Barajas[150], S. Cheatham[86], A. Chegwidden[89], S. Chekanov[6], S.V. Chekulaev[160a], G.A. Chelkov[64,h], M.A. Chelstowska[88], C. Chen[63], H. Chen[25], K. Chen[149], L. Chen[33d,i], S. Chen[33c], X. Chen[146c], Y. Chen[35], H.C. Cheng[88], Y. Cheng[31], A. Cheplakov[64], R. Cherkaoui El Moursli[136e], V. Chernyatin[25,*], E. Cheu[7], L. Chevalier[137], V. Chiarella[47], G. Chiefari[103a,103b], J.T. Childers[6], A. Chilingarov[71], G. Chiodini[72a], A.S. Chisholm[18], R.T. Chislett[77], A. Chitan[26a], M.V. Chizhov[64], S. Chouridou[9], B.K.B. Chow[99], D. Chromek-Burckhart[30], M.L. Chu[152], J. Chudoba[126], J.J. Chwastowski[39], L. Chytka[114], G. Ciapetti[133a,133b], A.K. Ciftci[4a], R. Ciftci[4a], D. Cinca[62], V. Cindro[74], A. Ciocio[15], P. Cirkovic[13b], Z.H. Citron[173], M. Citterio[90a], M. Ciubancan[26a], A. Clark[49], P.J. Clark[46], R.N. Clarke[15], W. Cleland[124], J.C. Clemens[84], C. Clement[147a,147b], Y. Coadou[84], M. Cobal[165a,165c], A. Coccaro[139], J. Cochran[63], L. Coffey[23], J.G. Cogan[144], J. Coggeshall[166], B. Cole[35], S. Cole[107], A.P. Colijn[106], J. Collot[55], T. Colombo[58c], G. Colon[85], G. Compostella[100], P. Conde Muiño[125a,125b], E. Coniavitis[167], M.C. Conidi[12], S.H. Connell[146b], I.A. Connelly[76], S.M. Consonni[90a,90b], V. Consorti[48], S. Constantinescu[26a], C. Conta[120a,120b], G. Conti[57], F. Conventi[103a,j], M. Cooke[15], B.D. Cooper[77], A.M. Cooper-Sarkar[119], N.J. Cooper-Smith[76], K. Copic[15], T. Cornelissen[176], M. Corradi[20a], F. Corriveau[86,k], A. Corso-Radu[164],

A. Cortes-Gonzalez[12], G. Cortiana[100], G. Costa[90a], M.J. Costa[168], D. Costanzo[140], D. Côté[8], G. Cottin[28], G. Cowan[76], B.E. Cox[83], K. Cranmer[109], G. Cree[29], S. Crépé-Renaudin[55], F. Crescioli[79], W.A. Cribbs[147a,147b], M. Crispin Ortuzar[119], M. Cristinziani[21], V. Croft[105], G. Crosetti[37a,37b], C.-M. Cuciuc[26a], T. Cuhadar Donszelmann[140], J. Cummings[177], M. Curatolo[47], C. Cuthbert[151], H. Czirr[142], P. Czodrowski[3], Z. Czyczula[177], S. D'Auria[53], M. D'Onofrio[73], M.J. Da Cunha Sargedas De Sousa[125a,125b], C. Da Via[83], W. Dabrowski[38a], A. Dafinca[119], T. Dai[88], O. Dale[14], F. Dallaire[94], C. Dallapiccola[85], M. Dam[36], A.C. Daniells[18], M. Dano Hoffmann[137], V. Dao[105], G. Darbo[50a], S. Darmora[8], J. Dassoulas[42], A. Dattagupta[60], W. Davey[21], C. David[170], T. Davidek[128], E. Davies[119,d], M. Davies[154], O. Davignon[79], A.R. Davison[77], P. Davison[77], Y. Davygora[58a], E. Dawe[143], I. Dawson[140], R.K. Daya-Ishmukhametova[85], K. De[8], R. de Asmundis[103a], S. De Castro[20a,20b], S. De Cecco[79], N. De Groot[105], P. de Jong[106], H. De la Torre[81], F. De Lorenzi[63], L. De Nooij[106], D. De Pedis[133a], A. De Salvo[133a], U. De Sanctis[165a,165b], A. De Santo[150], J.B. De Vivie De Regie[116], W.J. Dearnaley[71], R. Debbe[25], C. Debenedetti[46], B. Dechenaux[55], D.V. Dedovich[64], I. Deigaard[106], J. Del Peso[81], T. Del Prete[123a,123b], F. Deliot[137], C.M. Delitzsch[49], M. Deliyergiyev[74], A. Dell'Acqua[30], L. Dell'Asta[22], M. Dell'Orso[123a,123b], M. Della Pietra[103a,j], D. della Volpe[49], M. Delmastro[5], P.A. Delsart[55], C. Deluca[106], S. Demers[177], M. Demichev[64], A. Demilly[79], S.P. Denisov[129], D. Derendarz[39], J.E. Derkaoui[136d], F. Derue[79], P. Dervan[73], K. Desch[21], C. Deterre[42], P.O. Deviveiros[106], A. Dewhurst[130], S. Dhaliwal[106], A. Di Ciaccio[134a,134b], L. Di Ciaccio[5], A. Di Domenico[133a,133b], C. Di Donato[103a,103b], A. Di Girolamo[30], B. Di Girolamo[30], A. Di Mattia[153], B. Di Micco[135a,135b], R. Di Nardo[47], A. Di Simone[48], R. Di Sipio[20a,20b], D. Di Valentino[29], M.A. Diaz[32a], E.B. Diehl[88], J. Dietrich[42], T.A. Dietzsch[58a], S. Diglio[84], A. Dimitrievska[13a], J. Dingfelder[21], C. Dionisi[133a,133b], P. Dita[26a], S. Dita[26a], F. Dittus[30], F. Djama[84], T. Djobava[51b], J.I. Djuvsland[58a], M.A.B. do Vale[24c], A. Do Valle Wemans[125a,125g], T.K.O. Doan[5], D. Dobos[30], C. Doglioni[49], T. Doherty[53], T. Dohmae[156], J. Dolejsi[128], Z. Dolezal[128], B.A. Dolgoshein[97,*], M. Donadelli[24d], S. Donati[123a,123b], P. Dondero[120a,120b], J. Donini[34], J. Dopke[30], A. Doria[103a], M.T. Dova[70], A.T. Doyle[53], M. Dris[10], J. Dubbert[88], S. Dube[15], E. Dubreuil[34], E. Duchovni[173], G. Duckeck[99], O.A. Ducu[26a], D. Duda[176], A. Dudarev[30], F. Dudziak[63], L. Duflot[116], L. Duguid[76], M. Dührssen[30], M. Dunford[58a], H. Duran Yildiz[4a], M. Düren[52], A. Durglishvili[51b], M. Dwuznik[38a], M. Dyndal[38a], J. Ebke[99], W. Edson[2], N.C. Edwards[46], W. Ehrenfeld[21], T. Eifert[144], G. Eigen[14], K. Einsweiler[15], T. Ekelof[167], M. El Kacimi[136c], M. Ellert[167], S. Elles[5], F. Ellinghaus[82], N. Ellis[30], J. Elmsheuser[99], M. Elsing[30], D. Emeliyanov[130], Y. Enari[156], O.C. Endner[82], M. Endo[117], R. Engelmann[149], J. Erdmann[177], A. Ereditato[17], D. Eriksson[147a], G. Ernis[176], J. Ernst[2], M. Ernst[25], J. Ernwein[137], D. Errede[166], S. Errede[166], E. Ertel[82], M. Escalier[116], H. Esch[43], C. Escobar[124], B. Esposito[47], A.I. Etienvre[137], E. Etzion[154], H. Evans[60], A. Ezhilov[122], L. Fabbri[20a,20b], G. Facini[31], R.M. Fakhrutdinov[129], S. Falciano[133a], R.J. Falla[77], J. Faltova[128], Y. Fang[33a], M. Fanti[90a,90b], A. Farbin[8], A. Farilla[135a], T. Farooque[12], S. Farrell[164], S.M. Farrington[171], P. Farthouat[30], F. Fassi[136e], P. Fassnacht[30], D. Fassouliotis[9], A. Favareto[50a,50b], L. Fayard[116], P. Federic[145a], O.L. Fedin[122,l], W. Fedorko[169], M. Fehling-Kaschek[48], S. Feigl[30], L. Feligioni[84], C. Feng[33d], E.J. Feng[6], H. Feng[88], A.B. Fenyuk[129], S. Fernandez Perez[30], S. Ferrag[53], J. Ferrando[53], A. Ferrari[167], P. Ferrari[106], R. Ferrari[120a], D.E. Ferreira de Lima[53], A. Ferrer[168], D. Ferrere[49], C. Ferretti[88], A. Ferretto Parodi[50a,50b], M. Fiascaris[31], F. Fiedler[82], A. Filipčič[74], M. Filipuzzi[42], F. Filthaut[105], M. Fincke-Keeler[170], K.D. Finelli[151], M.C.N. Fiolhais[125a,125c], L. Fiorini[168], A. Firan[40], J. Fischer[176], W.C. Fisher[89], E.A. Fitzgerald[23], M. Flechl[48], I. Fleck[142], P. Fleischmann[88], S. Fleischmann[176], G.T. Fletcher[140], G. Fletcher[75], T. Flick[176], A. Floderus[80], L.R. Flores Castillo[174,m], A.C. Florez Bustos[160b], M.J. Flowerdew[100], A. Formica[137],

A. Forti[83], D. Fortin[160a], D. Fournier[116], H. Fox[71], S. Fracchia[12], P. Francavilla[79], M. Franchini[20a,20b], S. Franchino[30], D. Francis[30], M. Franklin[57], S. Franz[61], M. Fraternali[120a,120b], S.T. French[28], C. Friedrich[42], F. Friedrich[44], D. Froidevaux[30], J.A. Frost[28], C. Fukunaga[157], E. Fullana Torregrosa[82], B.G. Fulsom[144], J. Fuster[168], C. Gabaldon[55], O. Gabizon[173], A. Gabrielli[20a,20b], A. Gabrielli[133a,133b], S. Gadatsch[106], S. Gadomski[49], G. Gagliardi[50a,50b], P. Gagnon[60], C. Galea[105], B. Galhardo[125a,125c], E.J. Gallas[119], V. Gallo[17], B.J. Gallop[130], P. Gallus[127], G. Galster[36], K.K. Gan[110], R.P. Gandrajula[62], J. Gao[33b], Y.S. Gao[144,f], F.M. Garay Walls[46], F. Garberson[177], C. García[168], J.E. García Navarro[168], M. Garcia-Sciveres[15], R.W. Gardner[31], N. Garelli[144], V. Garonne[30], C. Gatti[47], G. Gaudio[120a], B. Gaur[142], L. Gauthier[94], P. Gauzzi[133a,133b], I.L. Gavrilenko[95], C. Gay[169], G. Gaycken[21], E.N. Gazis[10], P. Ge[33d], Z. Gecse[169], C.N.P. Gee[130], D.A.A. Geerts[106], Ch. Geich-Gimbel[21], K. Gellerstedt[147a,147b], C. Gemme[50a], A. Gemmell[53], M.H. Genest[55], S. Gentile[133a,133b], M. George[54], S. George[76], D. Gerbaudo[164], A. Gershon[154], H. Ghazlane[136b], N. Ghodbane[34], B. Giacobbe[20a], S. Giagu[133a,133b], V. Giangiobbe[12], P. Giannetti[123a,123b], F. Gianotti[30], B. Gibbard[25], S.M. Gibson[76], M. Gilchriese[15], T.P.S. Gillam[28], D. Gillberg[30], G. Gilles[34], D.M. Gingrich[3,e], N. Giokaris[9], M.P. Giordani[165a,165c], R. Giordano[103a,103b], F.M. Giorgi[20a], F.M. Giorgi[16], P.F. Giraud[137], D. Giugni[90a], C. Giuliani[48], M. Giulini[58b], B.K. Gjelsten[118], S. Gkaitatzis[155], I. Gkialas[155], L.K. Gladilin[98], C. Glasman[81], J. Glatzer[30], P.C.F. Glaysher[46], A. Glazov[42], G.L. Glonti[64], M. Goblirsch-Kolb[100], J.R. Goddard[75], J. Godfrey[143], J. Godlewski[30], C. Goeringer[82], S. Goldfarb[88], T. Golling[177], D. Golubkov[129], A. Gomes[125a,125b,125d], L.S. Gomez Fajardo[42], R. Gonçalo[125a], J. Goncalves Pinto Firmino Da Costa[137], L. Gonella[21], S. González de la Hoz[168], G. Gonzalez Parra[12], M.L. Gonzalez Silva[27], S. Gonzalez-Sevilla[49], L. Goossens[30], P.A. Gorbounov[96], H.A. Gordon[25], I. Gorelov[104], B. Gorini[30], E. Gorini[72a,72b], A. Gorišek[74], E. Gornicki[39], A.T. Goshaw[6], C. Gössling[43], M.I. Gostkin[64], M. Gouighri[136a], D. Goujdami[136c], M.P. Goulette[49], A.G. Goussiou[139], C. Goy[5], S. Gozpinar[23], H.M.X. Grabas[137], L. Graber[54], I. Grabowska-Bold[38a], P. Grafström[20a,20b], K-J. Grahn[42], J. Gramling[49], E. Gramstad[118], S. Grancagnolo[16], V. Grassi[149], V. Gratchev[122], H.M. Gray[30], E. Graziani[135a], O.G. Grebenyuk[122], Z.D. Greenwood[78,n], K. Gregersen[77], I.M. Gregor[42], P. Grenier[144], J. Griffiths[8], A.A. Grillo[138], K. Grimm[71], S. Grinstein[12,o], Ph. Gris[34], Y.V. Grishkevich[98], J.-F. Grivaz[116], J.P. Grohs[44], A. Grohsjean[42], E. Gross[173], J. Grosse-Knetter[54], G.C. Grossi[134a,134b], J. Groth-Jensen[173], Z.J. Grout[150], L. Guan[33b], J. Guenther[127], F. Guescini[49], D. Guest[177], O. Gueta[154], C. Guicheney[34], E. Guido[50a,50b], T. Guillemin[116], S. Guindon[2], U. Gul[53], C. Gumpert[44], J. Guo[35], S. Gupta[119], P. Gutierrez[112], N.G. Gutierrez Ortiz[53], C. Gutschow[77], N. Guttman[154], C. Guyot[137], C. Gwenlan[119], C.B. Gwilliam[73], A. Haas[109], C. Haber[15], H.K. Hadavand[8], N. Haddad[136e], P. Haefner[21], S. Hageböck[21], Z. Hajduk[39], H. Hakobyan[178], M. Haleem[42], D. Hall[119], G. Halladjian[89], K. Hamacher[176], P. Hamal[114], K. Hamano[170], M. Hamer[54], A. Hamilton[146a], S. Hamilton[162], P.G. Hamnett[42], L. Han[33b], K. Hanagaki[117], K. Hanawa[156], M. Hance[15], P. Hanke[58a], R. Hanna[137], J.B. Hansen[36], J.D. Hansen[36], P.H. Hansen[36], K. Hara[161], A.S. Hard[174], T. Harenberg[176], F. Hariri[116], S. Harkusha[91], D. Harper[88], R.D. Harrington[46], O.M. Harris[139], P.F. Harrison[171], F. Hartjes[106], S. Hasegawa[102], Y. Hasegawa[141], A. Hasib[112], S. Hassani[137], S. Haug[17], M. Hauschild[30], R. Hauser[89], M. Havranek[126], C.M. Hawkes[18], R.J. Hawkings[30], A.D. Hawkins[80], T. Hayashi[161], D. Hayden[89], C.P. Hays[119], H.S. Hayward[73], S.J. Haywood[130], S.J. Head[18], T. Heck[82], V. Hedberg[80], L. Heelan[8], S. Heim[121], T. Heim[176], B. Heinemann[15], L. Heinrich[109], S. Heisterkamp[36], J. Hejbal[126], L. Helary[22], C. Heller[99], M. Heller[30], S. Hellman[147a,147b], D. Hellmich[21], C. Helsens[30], J. Henderson[119], R.C.W. Henderson[71], C. Hengler[42], A. Henrichs[177], A.M. Henriques Correia[30], S. Henrot-Versille[116], C. Hensel[54], G.H. Herbert[16], Y. Hernández Jiménez[168], R. Herrberg-Schubert[16],

G. Herten[48], R. Hertenberger[99], L. Hervas[30], G.G. Hesketh[77], N.P. Hessey[106], R. Hickling[75], E. Higón-Rodriguez[168], E. Hill[170], J.C. Hill[28], K.H. Hiller[42], S. Hillert[21], S.J. Hillier[18], I. Hinchliffe[15], E. Hines[121], M. Hirose[158], D. Hirschbuehl[176], J. Hobbs[149], N. Hod[106], M.C. Hodgkinson[140], P. Hodgson[140], A. Hoecker[30], M.R. Hoeferkamp[104], J. Hoffman[40], D. Hoffmann[84], M. Hohlfeld[82], T.R. Holmes[15], T.M. Hong[121], L. Hooft van Huysduynen[109], J-Y. Hostachy[55], S. Hou[152], A. Hoummada[136a], J. Howard[119], J. Howarth[42], M. Hrabovsky[114], I. Hristova[16], J. Hrivnac[116], T. Hryn'ova[5], P.J. Hsu[82], S.-C. Hsu[139], D. Hu[35], X. Hu[88], Y. Huang[42], Z. Hubacek[30], F. Hubaut[84], F. Huegging[21], T.B. Huffman[119], E.W. Hughes[35], G. Hughes[71], M. Huhtinen[30], T.A. Hülsing[82], M. Hurwitz[15], N. Huseynov[64,b], J. Huston[89], J. Huth[57], G. Iacobucci[49], G. Iakovidis[10], I. Ibragimov[142], L. Iconomidou-Fayard[116], E. Ideal[177], P. Iengo[103a], O. Igonkina[106], T. Iizawa[172], Y. Ikegami[65], K. Ikematsu[142], M. Ikeno[65], Y. Ilchenko[31,p], D. Iliadis[155], N. Ilic[159], Y. Inamaru[66], T. Ince[100], P. Ioannou[9], M. Iodice[135a], K. Iordanidou[9], V. Ippolito[57], A. Irles Quiles[168], C. Isaksson[167], M. Ishino[67], M. Ishitsuka[158], R. Ishmukhametov[110], C. Issever[119], S. Istin[19a], J.M. Iturbe Ponce[83], R. Iuppa[134a,134b], J. Ivarsson[80], W. Iwanski[39], H. Iwasaki[65], J.M. Izen[41], V. Izzo[103a], B. Jackson[121], M. Jackson[73], P. Jackson[1], M.R. Jaekel[30], V. Jain[2], K. Jakobs[48], S. Jakobsen[30], T. Jakoubek[126], J. Jakubek[127], D.O. Jamin[152], D.K. Jana[78], E. Jansen[77], H. Jansen[30], J. Janssen[21], M. Janus[171], G. Jarlskog[80], N. Javadov[64,b], T. Javůrek[48], L. Jeanty[15], J. Jejelava[51a,q], G.-Y. Jeng[151], D. Jennens[87], P. Jenni[48,r], J. Jentzsch[43], C. Jeske[171], S. Jézéquel[5], H. Ji[174], W. Ji[82], J. Jia[149], Y. Jiang[33b], M. Jimenez Belenguer[42], S. Jin[33a], A. Jinaru[26a], O. Jinnouchi[158], M.D. Joergensen[36], K.E. Johansson[147a], P. Johansson[140], K.A. Johns[7], K. Jon-And[147a,147b], G. Jones[171], R.W.L. Jones[71], T.J. Jones[73], J. Jongmanns[58a], P.M. Jorge[125a,125b], K.D. Joshi[83], J. Jovicevic[148], X. Ju[174], C.A. Jung[43], R.M. Jungst[30], P. Jussel[61], A. Juste Rozas[12,o], M. Kaci[168], A. Kaczmarska[39], M. Kado[116], H. Kagan[110], M. Kagan[144], E. Kajomovitz[45], C.W. Kalderon[119], S. Kama[40], N. Kanaya[156], M. Kaneda[30], S. Kaneti[28], T. Kanno[158], V.A. Kantserov[97], J. Kanzaki[65], B. Kaplan[109], A. Kapliy[31], D. Kar[53], K. Karakostas[10], N. Karastathis[10], M. Karnevskiy[82], S.N. Karpov[64], Z.M. Karpova[64], K. Karthik[109], V. Kartvelishvili[71], A.N. Karyukhin[129], L. Kashif[174], G. Kasieczka[58b], R.D. Kass[110], A. Kastanas[14], Y. Kataoka[156], A. Katre[49], J. Katzy[42], V. Kaushik[7], K. Kawagoe[69], T. Kawamoto[156], G. Kawamura[54], S. Kazama[156], V.F. Kazanin[108], M.Y. Kazarinov[64], R. Keeler[170], R. Kehoe[40], M. Keil[54], J.S. Keller[42], J.J. Kempster[76], H. Keoshkerian[5], O. Kepka[126], B.P. Kerševan[74], S. Kersten[176], K. Kessoku[156], J. Keung[159], F. Khalil-zada[11], H. Khandanyan[147a,147b], A. Khanov[113], A. Khodinov[97], A. Khomich[58a], T.J. Khoo[28], G. Khoriauli[21], A. Khoroshilov[176], V. Khovanskiy[96], E. Khramov[64], J. Khubua[51b], H.Y. Kim[8], H. Kim[147a,147b], S.H. Kim[161], N. Kimura[172], O. Kind[16], B.T. King[73], M. King[168], R.S.B. King[119], S.B. King[169], J. Kirk[130], A.E. Kiryunin[100], T. Kishimoto[66], D. Kisielewska[38a], F. Kiss[48], T. Kitamura[66], T. Kittelmann[124], K. Kiuchi[161], E. Kladiva[145b], M. Klein[73], U. Klein[73], K. Kleinknecht[82], P. Klimek[147a,147b], A. Klimentov[25], R. Klingenberg[43], J.A. Klinger[83], T. Klioutchnikova[30], P.F. Klok[105], E.-E. Kluge[58a], P. Kluit[106], S. Kluth[100], E. Kneringer[61], E.B.F.G. Knoops[84], A. Knue[53], T. Kobayashi[156], M. Kobel[44], M. Kocian[144], P. Kodys[128], P. Koevesarki[21], T. Koffas[29], E. Koffeman[106], L.A. Kogan[119], S. Kohlmann[176], Z. Kohout[127], T. Kohriki[65], T. Koi[144], H. Kolanoski[16], I. Koletsou[5], J. Koll[89], A.A. Komar[95,*], Y. Komori[156], T. Kondo[65], N. Kondrashova[42], K. Köneke[48], A.C. König[105], S. König[82], T. Kono[65,s], R. Konoplich[109,t], N. Konstantinidis[77], R. Kopeliansky[153], S. Koperny[38a], L. Köpke[82], A.K. Kopp[48], K. Korcyl[39], K. Kordas[155], A. Korn[77], A.A. Korol[108,c], I. Korolkov[12], E.V. Korolkova[140], V.A. Korotkov[129], O. Kortner[100], S. Kortner[100], V.V. Kostyukhin[21], V.M. Kotov[64], A. Kotwal[45], C. Kourkoumelis[9], V. Kouskoura[155], A. Koutsman[160a], R. Kowalewski[170], T.Z. Kowalski[38a], W. Kozanecki[137], A.S. Kozhin[129], V. Kral[127], V.A. Kramarenko[98], G. Kramberger[74], D. Krasnopevtsev[97], M.W. Krasny[79],

JHEP09(2015)049

A. Krasznahorkay[30], J.K. Kraus[21], A. Kravchenko[25], S. Kreiss[109], M. Kretz[58c], J. Kretzschmar[73], K. Kreutzfeldt[52], P. Krieger[159], K. Kroeninger[54], H. Kroha[100], J. Kroll[121], J. Kroseberg[21], J. Krstic[13a], U. Kruchonak[64], H. Krüger[21], T. Kruker[17], N. Krumnack[63], Z.V. Krumshteyn[64], A. Kruse[174], M.C. Kruse[45], M. Kruskal[22], T. Kubota[87], S. Kuday[4a], S. Kuehn[48], A. Kugel[58c], A. Kuhl[138], T. Kuhl[42], V. Kukhtin[64], Y. Kulchitsky[91], S. Kuleshov[32b], M. Kuna[133a,133b], J. Kunkle[121], A. Kupco[126], H. Kurashige[66], Y.A. Kurochkin[91], R. Kurumida[66], V. Kus[126], E.S. Kuwertz[148], M. Kuze[158], J. Kvita[114], A. La Rosa[49], L. La Rotonda[37a,37b], C. Lacasta[168], F. Lacava[133a,133b], J. Lacey[29], H. Lacker[16], D. Lacour[79], V.R. Lacuesta[168], E. Ladygin[64], R. Lafaye[5], B. Laforge[79], T. Lagouri[177], S. Lai[48], H. Laier[58a], L. Lambourne[77], S. Lammers[60], C.L. Lampen[7], W. Lampl[7], E. Lançon[137], U. Landgraf[48], M.P.J. Landon[75], V.S. Lang[58a], C. Lange[42], A.J. Lankford[164], F. Lanni[25], K. Lantzsch[30], S. Laplace[79], C. Lapoire[21], J.F. Laporte[137], T. Lari[90a], M. Lassnig[30], P. Laurelli[47], W. Lavrijsen[15], A.T. Law[138], P. Laycock[73], B.T. Le[55], O. Le Dortz[79], E. Le Guirriec[84], E. Le Menedeu[12], T. LeCompte[6], F. Ledroit-Guillon[55], C.A. Lee[152], H. Lee[106], J.S.H. Lee[117], S.C. Lee[152], L. Lee[177], G. Lefebvre[79], M. Lefebvre[170], F. Legger[99], C. Leggett[15], A. Lehan[73], M. Lehmacher[21], G. Lehmann Miotto[30], X. Lei[7], W.A. Leight[29], A. Leisos[155], A.G. Leister[177], M.A.L. Leite[24d], R. Leitner[128], D. Lellouch[173], B. Lemmer[54], K.J.C. Leney[77], T. Lenz[106], G. Lenzen[176], B. Lenzi[30], R. Leone[7], K. Leonhardt[44], S. Leontsinis[10], C. Leroy[94], C.G. Lester[28], C.M. Lester[121], M. Levchenko[122], J. Levêque[5], D. Levin[88], L.J. Levinson[173], M. Levy[18], A. Lewis[119], G.H. Lewis[109], A.M. Leyko[21], M. Leyton[41], B. Li[33b,u], B. Li[84], H. Li[149], H.L. Li[31], L. Li[45], L. Li[33e], S. Li[45], Y. Li[33c,v], Z. Liang[138], H. Liao[34], B. Liberti[134a], P. Lichard[30], K. Lie[166], J. Liebal[21], W. Liebig[14], C. Limbach[21], A. Limosani[87], S.C. Lin[152,w], T.H. Lin[82], F. Linde[106], B.E. Lindquist[149], J.T. Linnemann[89], E. Lipeles[121], A. Lipniacka[14], M. Lisovyi[42], T.M. Liss[166], D. Lissauer[25], A. Lister[169], A.M. Litke[138], B. Liu[152], D. Liu[152], J.B. Liu[33b], K. Liu[33b,x], L. Liu[88], M. Liu[45], M. Liu[33b], Y. Liu[33b], M. Livan[120a,120b], S.S.A. Livermore[119], A. Lleres[55], J. Llorente Merino[81], S.L. Lloyd[75], F. Lo Sterzo[152], E. Lobodzinska[42], P. Loch[7], W.S. Lockman[138], F.K. Loebinger[83], A.E. Loevschall-Jensen[36], A. Loginov[177], C.W. Loh[169], T. Lohse[16], K. Lohwasser[42], M. Lokajicek[126], V.P. Lombardo[5], B.A. Long[22], J.D. Long[88], R.E. Long[71], L. Lopes[125a], D. Lopez Mateos[57], B. Lopez Paredes[140], I. Lopez Paz[12], J. Lorenz[99], N. Lorenzo Martinez[60], M. Losada[163], P. Loscutoff[15], X. Lou[41], A. Lounis[116], J. Love[6], P.A. Love[71], A.J. Lowe[144,f], F. Lu[33a], H.J. Lubatti[139], C. Luci[133a,133b], A. Lucotte[55], F. Luehring[60], W. Lukas[61], L. Luminari[133a], O. Lundberg[147a,147b], B. Lund-Jensen[148], M. Lungwitz[82], D. Lynn[25], R. Lysak[126], E. Lytken[80], H. Ma[25], L.L. Ma[33d], G. Maccarrone[47], A. Macchiolo[100], J. Machado Miguens[125a,125b], D. Macina[30], D. Madaffari[84], R. Madar[48], H.J. Maddocks[71], W.F. Mader[44], A. Madsen[167], M. Maeno[8], T. Maeno[25], E. Magradze[54], K. Mahboubi[48], J. Mahlstedt[106], S. Mahmoud[73], C. Maiani[137], C. Maidantchik[24a], A. Maio[125a,125b,125d], S. Majewski[115], Y. Makida[65], N. Makovec[116], P. Mal[137,y], B. Malaescu[79], Pa. Malecki[39], V.P. Maleev[122], F. Malek[55], U. Mallik[62], D. Malon[6], C. Malone[144], S. Maltezos[10], V.M. Malyshev[108], S. Malyukov[30], J. Mamuzic[13b], B. Mandelli[30], L. Mandelli[90a], I. Mandić[74], R. Mandrysch[62], J. Maneira[125a,125b], A. Manfredini[100], L. Manhaes de Andrade Filho[24b], J.A. Manjarres Ramos[160b], A. Mann[99], P.M. Manning[138], A. Manousakis-Katsikakis[9], B. Mansoulie[137], R. Mantifel[86], L. Mapelli[30], L. March[168], J.F. Marchand[29], G. Marchiori[79], M. Marcisovsky[126], C.P. Marino[170], M. Marjanovic[13a], C.N. Marques[125a], F. Marroquim[24a], S.P. Marsden[83], Z. Marshall[15], L.F. Marti[17], S. Marti-Garcia[168], B. Martin[30], B. Martin[89], T.A. Martin[171], V.J. Martin[46], B. Martin dit Latour[14], H. Martinez[137], M. Martinez[12,o], S. Martin-Haugh[130], A.C. Martyniuk[77], M. Marx[139], F. Marzano[133a], A. Marzin[30], L. Masetti[82], T. Mashimo[156], R. Mashinistov[95], J. Masik[83], A.L. Maslennikov[108,c], I. Massa[20a,20b], N. Massol[5], P. Mastrandrea[149],

A. Mastroberardino[37a,37b], T. Masubuchi[156], T. Matsushita[66], P. Mättig[176], S. Mättig[42], J. Mattmann[82], J. Maurer[26a], S.J. Maxfield[73], D.A. Maximov[108,c], R. Mazini[152], L. Mazzaferro[134a,134b], G. Mc Goldrick[159], S.P. Mc Kee[88], A. McCarn[88], R.L. McCarthy[149], T.G. McCarthy[29], N.A. McCubbin[130], K.W. McFarlane[56,*], J.A. Mcfayden[77], G. Mchedlidze[54], S.J. McMahon[130], R.A. McPherson[170,k], A. Meade[85], J. Mechnich[106], M. Medinnis[42], S. Meehan[31], S. Mehlhase[36], A. Mehta[73], K. Meier[58a], C. Meineck[99], B. Meirose[80], C. Melachrinos[31], B.R. Mellado Garcia[146c], F. Meloni[90a,90b], A. Mengarelli[20a,20b], S. Menke[100], E. Meoni[162], K.M. Mercurio[57], S. Mergelmeyer[21], N. Meric[137], P. Mermod[49], L. Merola[103a,103b], C. Meroni[90a], F.S. Merritt[31], H. Merritt[110], A. Messina[30,z], J. Metcalfe[25], A.S. Mete[164], C. Meyer[82], C. Meyer[31], J-P. Meyer[137], J. Meyer[30], R.P. Middleton[130], S. Migas[73], L. Mijović[21], G. Mikenberg[173], M. Mikestikova[126], M. Mikuž[74], A. Milic[30], D.W. Miller[31], C. Mills[46], A. Milov[173], D.A. Milstead[147a,147b], D. Milstein[173], A.A. Minaenko[129], I.A. Minashvili[64], A.I. Mincer[109], B. Mindur[38a], M. Mineev[64], Y. Ming[174], L.M. Mir[12], G. Mirabelli[133a], T. Mitani[172], J. Mitrevski[99], V.A. Mitsou[168], S. Mitsui[65], A. Miucci[49], P.S. Miyagawa[140], J.U. Mjörnmark[80], T. Moa[147a,147b], K. Mochizuki[84], V. Moeller[28], S. Mohapatra[35], W. Mohr[48], S. Molander[147a,147b], R. Moles-Valls[168], K. Mönig[42], C. Monini[55], J. Monk[36], E. Monnier[84], J. Montejo Berlingen[12], F. Monticelli[70], S. Monzani[133a,133b], R.W. Moore[3], A. Moraes[53], N. Morange[62], D. Moreno[82], M. Moreno Llácer[54], P. Morettini[50a], M. Morgenstern[44], M. Morii[57], S. Moritz[82], A.K. Morley[148], G. Mornacchi[30], J.D. Morris[75], L. Morvaj[102], H.G. Moser[100], M. Mosidze[51b], J. Moss[110], R. Mount[144], E. Mountricha[25], S.V. Mouraviev[95,*], E.J.W. Moyse[85], S. Muanza[84], R.D. Mudd[18], F. Mueller[58a], J. Mueller[124], K. Mueller[21], T. Mueller[28], T. Mueller[82], D. Muenstermann[49], Y. Munwes[154], J.A. Murillo Quijada[18], W.J. Murray[171,130], H. Musheghyan[54], E. Musto[153], A.G. Myagkov[129,aa], M. Myska[127], O. Nackenhorst[54], J. Nadal[54], K. Nagai[61], R. Nagai[158], Y. Nagai[84], K. Nagano[65], A. Nagarkar[110], Y. Nagasaka[59], M. Nagel[100], A.M. Nairz[30], Y. Nakahama[30], K. Nakamura[65], T. Nakamura[156], I. Nakano[111], H. Namasivayam[41], G. Nanava[21], R. Narayan[58b], T. Nattermann[21], T. Naumann[42], G. Navarro[163], R. Nayyar[7], H.A. Neal[88], P.Yu. Nechaeva[95], T.J. Neep[83], A. Negri[120a,120b], G. Negri[30], M. Negrini[20a], S. Nektarijevic[49], A. Nelson[164], T.K. Nelson[144], S. Nemecek[126], P. Nemethy[109], A.A. Nepomuceno[24a], M. Nessi[30,ab], M.S. Neubauer[166], M. Neumann[176], R.M. Neves[109], P. Nevski[25], P.R. Newman[18], D.H. Nguyen[6], R.B. Nickerson[119], R. Nicolaidou[137], B. Nicquevert[30], J. Nielsen[138], N. Nikiforou[35], A. Nikiforov[16], V. Nikolaenko[129,aa], I. Nikolic-Audit[79], K. Nikolics[49], K. Nikolopoulos[18], P. Nilsson[8], Y. Ninomiya[156], A. Nisati[133a], R. Nisius[100], T. Nobe[158], L. Nodulman[6], M. Nomachi[117], I. Nomidis[155], S. Norberg[112], M. Nordberg[30], S. Nowak[100], M. Nozaki[65], L. Nozka[114], K. Ntekas[10], G. Nunes Hanninger[87], T. Nunnemann[99], E. Nurse[77], F. Nuti[87], B.J. O'Brien[46], F. O'grady[7], D.C. O'Neil[143], V. O'Shea[53], F.G. Oakham[29,e], H. Oberlack[100], T. Obermann[21], J. Ocariz[79], A. Ochi[66], I. Ochoa[77], S. Oda[69], S. Odaka[65], H. Ogren[60], A. Oh[83], S.H. Oh[45], C.C. Ohm[30], H. Ohman[167], T. Ohshima[102], W. Okamura[117], H. Okawa[25], Y. Okumura[31], T. Okuyama[156], A. Olariu[26a], A.G. Olchevski[64], S.A. Olivares Pino[46], D. Oliveira Damazio[25], E. Oliver Garcia[168], A. Olszewski[39], J. Olszowska[39], A. Onofre[125a,125e], P.U.E. Onyisi[31,p], C.J. Oram[160a], M.J. Oreglia[31], Y. Oren[154], D. Orestano[135a,135b], N. Orlando[72a,72b], C. Oropeza Barrera[53], R.S. Orr[159], B. Osculati[50a,50b], R. Ospanov[121], G. Otero y Garzon[27], H. Otono[69], M. Ouchrif[136d], E.A. Ouellette[170], F. Ould-Saada[118], A. Ouraou[137], K.P. Oussoren[106], Q. Ouyang[33a], A. Ovcharova[15], M. Owen[83], V.E. Ozcan[19a], N. Ozturk[8], K. Pachal[119], A. Pacheco Pages[12], C. Padilla Aranda[12], M. Pagáčová[48], S. Pagan Griso[15], E. Paganis[140], C. Pahl[100], F. Paige[25], P. Pais[85], K. Pajchel[118], G. Palacino[160b], S. Palestini[30], M. Palka[38b], D. Pallin[34], A. Palma[125a,125b], J.D. Palmer[18], Y.B. Pan[174], E. Panagiotopoulou[10], J.G. Panduro Vazquez[76], P. Pani[106], N. Panikashvili[88],

JHEP09(2015)049

S. Panitkin[25], D. Pantea[26a], L. Paolozzi[134a,134b], Th.D. Papadopoulou[10],
K. Papageorgiou[155], A. Paramonov[6], D. Paredes Hernandez[34], M.A. Parker[28],
F. Parodi[50a,50b], J.A. Parsons[35], U. Parzefall[48], E. Pasqualucci[133a], S. Passaggio[50a],
A. Passeri[135a], F. Pastore[135a,135b,*], Fr. Pastore[76], G. Pásztor[29], S. Pataraia[176],
N.D. Patel[151], J.R. Pater[83], S. Patricelli[103a,103b], T. Pauly[30], J. Pearce[170],
M. Pedersen[118], S. Pedraza Lopez[168], R. Pedro[125a,125b], S.V. Peleganchuk[108],
D. Pelikan[167], H. Peng[33b], B. Penning[31], J. Penwell[60], D.V. Perepelitsa[25],
E. Perez Codina[160a], M.T. Pérez García-Estañ[168], V. Perez Reale[35], L. Perini[90a,90b],
H. Pernegger[30], R. Perrino[72a], R. Peschke[42], V.D. Peshekhonov[64], K. Peters[30],
R.F.Y. Peters[83], B.A. Petersen[30], T.C. Petersen[36], E. Petit[42], A. Petridis[147a,147b],
C. Petridou[155], E. Petrolo[133a], F. Petrucci[135a,135b], M. Petteni[143], N.E. Pettersson[158],
R. Pezoa[32b], P.W. Phillips[130], G. Piacquadio[144], E. Pianori[171], A. Picazio[49], E. Piccaro[75],
M. Piccinini[20a,20b], R. Piegaia[27], D.T. Pignotti[110], J.E. Pilcher[31], A.D. Pilkington[77],
J. Pina[125a,125b,125d], M. Pinamonti[165a,165c,ac], A. Pinder[119], J.L. Pinfold[3], A. Pingel[36],
B. Pinto[125a], S. Pires[79], M. Pitt[173], C. Pizio[90a,90b], L. Plazak[145a], M.-A. Pleier[25],
V. Pleskot[128], E. Plotnikova[64], P. Plucinski[147a,147b], S. Poddar[58a], F. Podlyski[34],
R. Poettgen[82], L. Poggioli[116], D. Pohl[21], M. Pohl[49], G. Polesello[120a], A. Policicchio[37a,37b],
R. Polifka[159], A. Polini[20a], C.S. Pollard[45], V. Polychronakos[25], K. Pommès[30],
L. Pontecorvo[133a], B.G. Pope[89], G.A. Popeneciu[26b], D.S. Popovic[13a], A. Poppleton[30],
X. Portell Bueso[12], G.E. Pospelov[100], S. Pospisil[127], K. Potamianos[15], I.N. Potrap[64],
C.J. Potter[150], C.T. Potter[115], G. Poulard[30], J. Poveda[60], V. Pozdnyakov[64],
P. Pralavorio[84], A. Pranko[15], S. Prasad[30], R. Pravahan[8], S. Prell[63], D. Price[83], J. Price[73],
L.E. Price[6], D. Prieur[124], M. Primavera[72a], M. Proissl[46], K. Prokofiev[47], F. Prokoshin[32b],
E. Protopapadaki[137], S. Protopopescu[25], J. Proudfoot[6], M. Przybycien[38a],
H. Przysiezniak[5], E. Ptacek[115], E. Pueschel[85], D. Puldon[149], M. Purohit[25,ad], P. Puzo[116],
J. Qian[88], G. Qin[53], Y. Qin[83], A. Quadt[54], D.R. Quarrie[15], W.B. Quayle[165a,165b],
M. Queitsch-Maitland[83], D. Quilty[53], A. Qureshi[160b], V. Radeka[25], V. Radescu[42],
S.K. Radhakrishnan[149], P. Radloff[115], P. Rados[87], F. Ragusa[90a,90b], G. Rahal[179],
S. Rajagopalan[25], M. Rammensee[30], A.S. Randle-Conde[40], C. Rangel-Smith[167],
K. Rao[164], F. Rauscher[99], T.C. Rave[48], T. Ravenscroft[53], M. Raymond[30], A.L. Read[118],
N.P. Readioff[73], D.M. Rebuzzi[120a,120b], A. Redelbach[175], G. Redlinger[25], R. Reece[138],
K. Reeves[41], L. Rehnisch[16], H. Reisin[27], M. Relich[164], C. Rembser[30], H. Ren[33a],
Z.L. Ren[152], A. Renaud[116], M. Rescigno[133a], S. Resconi[90a], O.L. Rezanova[108,c],
P. Reznicek[128], R. Rezvani[94], R. Richter[100], E. Richter-Was[38b], M. Ridel[79], P. Rieck[16],
J. Rieger[54], M. Rijssenbeek[149], A. Rimoldi[120a,120b], L. Rinaldi[20a], E. Ritsch[61], I. Riu[12],
F. Rizatdinova[113], E. Rizvi[75], S.H. Robertson[86,k], A. Robichaud-Veronneau[86],
D. Robinson[28], J.E.M. Robinson[83], A. Robson[53], C. Roda[123a,123b], L. Rodrigues[30],
S. Roe[30], O. Røhne[118], S. Rolli[162], A. Romaniouk[97], M. Romano[20a,20b], G. Romeo[27],
E. Romero Adam[168], N. Rompotis[139], L. Roos[79], E. Ros[168], S. Rosati[133a], K. Rosbach[49],
M. Rose[76], P.L. Rosendahl[14], O. Rosenthal[142], V. Rossetti[147a,147b], E. Rossi[103a,103b],
L.P. Rossi[50a], R. Rosten[139], M. Rotaru[26a], I. Roth[173], J. Rothberg[139], D. Rousseau[116],
C.R. Royon[137], A. Rozanov[84], Y. Rozen[153], X. Ruan[146c], F. Rubbo[12], I. Rubinskiy[42],
V.I. Rud[98], C. Rudolph[44], M.S. Rudolph[159], F. Rühr[48], A. Ruiz-Martinez[30],
Z. Rurikova[48], N.A. Rusakovich[64], A. Ruschke[99], J.P. Rutherfoord[7], N. Ruthmann[48],
Y.F. Ryabov[122], M. Rybar[128], G. Rybkin[116], N.C. Ryder[119], A.F. Saavedra[151],
S. Sacerdoti[27], A. Saddique[3], I. Sadeh[154], H.F-W. Sadrozinski[138], R. Sadykov[64],
F. Safai Tehrani[133a], H. Sakamoto[156], Y. Sakurai[172], G. Salamanna[75], A. Salamon[134a],
M. Saleem[112], D. Salek[106], P.H. Sales De Bruin[139], D. Salihagic[100], A. Salnikov[144],
J. Salt[168], B.M. Salvachua Ferrando[6], D. Salvatore[37a,37b], F. Salvatore[150], A. Salvucci[105],
A. Salzburger[30], D. Sampsonidis[155], A. Sanchez[103a,103b], J. Sánchez[168],
V. Sanchez Martinez[168], H. Sandaker[14], R.L. Sandbach[75], H.G. Sander[82], M.P. Sanders[99],
M. Sandhoff[176], T. Sandoval[28], C. Sandoval[163], R. Sandstroem[100], D.P.C. Sankey[130],

JHEP09(2015)049

A. Sansoni[47], C. Santoni[34], R. Santonico[134a,134b], H. Santos[125a], I. Santoyo Castillo[150], K. Sapp[124], A. Sapronov[64], J.G. Saraiva[125a,125d], B. Sarrazin[21], G. Sartisohn[176], O. Sasaki[65], Y. Sasaki[156], G. Sauvage[5,*], E. Sauvan[5], P. Savard[159,e], D.O. Savu[30], C. Sawyer[119], L. Sawyer[78,n], D.H. Saxon[53], J. Saxon[121], C. Sbarra[20a], A. Sbrizzi[3], T. Scanlon[77], D.A. Scannicchio[164], M. Scarcella[151], J. Schaarschmidt[173], P. Schacht[100], D. Schaefer[121], R. Schaefer[42], S. Schaepe[21], S. Schaetzel[58b], U. Schäfer[82], A.C. Schaffer[116], D. Schaile[99], R.D. Schamberger[149], V. Scharf[58a], V.A. Schegelsky[122], D. Scheirich[128], M. Schernau[164], M.I. Scherzer[35], C. Schiavi[50a,50b], J. Schieck[99], C. Schillo[48], M. Schioppa[37a,37b], S. Schlenker[30], E. Schmidt[48], K. Schmieden[30], C. Schmitt[82], S. Schmitt[58b], B. Schneider[17], Y.J. Schnellbach[73], U. Schnoor[44], L. Schoeffel[137], A. Schoening[58b], B.D. Schoenrock[89], A.L.S. Schorlemmer[54], M. Schott[82], D. Schouten[160a], J. Schovancova[25], S. Schramm[159], M. Schreyer[175], C. Schroeder[82], N. Schuh[82], M.J. Schultens[21], H.-C. Schultz-Coulon[58a], H. Schulz[16], M. Schumacher[48], B.A. Schumm[138], Ph. Schune[137], C. Schwanenberger[83], A. Schwartzman[144], Ph. Schwegler[100], Ph. Schwemling[137], R. Schwienhorst[89], J. Schwindling[137], T. Schwindt[21], M. Schwoerer[5], F.G. Sciacca[17], E. Scifo[116], G. Sciolla[23], W.G. Scott[130], F. Scuri[123a,123b], F. Scutti[21], J. Searcy[88], G. Sedov[42], E. Sedykh[122], S.C. Seidel[104], A. Seiden[138], F. Seifert[127], J.M. Seixas[24a], G. Sekhniaidze[103a], S.J. Sekula[40], K.E. Selbach[46], D.M. Seliverstov[122,*], G. Sellers[73], N. Semprini-Cesari[20a,20b], C. Serfon[30], L. Serin[116], L. Serkin[54], T. Serre[84], R. Seuster[160a], H. Severini[112], F. Sforza[100], A. Sfyrla[30], E. Shabalina[54], M. Shamim[115], L.Y. Shan[33a], R. Shang[166], J.T. Shank[22], Q.T. Shao[87], M. Shapiro[15], P.B. Shatalov[96], K. Shaw[165a,165b], P. Sherwood[77], L. Shi[152,ae], S. Shimizu[66], C.O. Shimmin[164], M. Shimojima[101], M. Shiyakova[64], A. Shmeleva[95], M.J. Shochet[31], D. Short[119], S. Shrestha[63], E. Shulga[97], M.A. Shupe[7], S. Shushkevich[42], P. Sicho[126], O. Sidiropoulou[155], D. Sidorov[113], A. Sidoti[133a], F. Siegert[44], Dj. Sijacki[13a], J. Silva[125a,125d], Y. Silver[154], D. Silverstein[144], S.B. Silverstein[147a], V. Simak[127], O. Simard[5], Lj. Simic[13a], S. Simion[116], E. Simioni[82], B. Simmons[77], R. Simoniello[90a,90b], M. Simonyan[36], P. Sinervo[159], N.B. Sinev[115], V. Sipica[142], G. Siragusa[175], A. Sircar[78], A.N. Sisakyan[64,*], S.Yu. Sivoklokov[98], J. Sjölin[147a,147b], T.B. Sjursen[14], H.P. Skottowe[57], K.Yu. Skovpen[108], P. Skubic[112], M. Slater[18], T. Slavicek[127], K. Sliwa[162], V. Smakhtin[173], B.H. Smart[46], L. Smestad[14], S.Yu. Smirnov[97], Y. Smirnov[97], L.N. Smirnova[98,af], O. Smirnova[80], K.M. Smith[53], M. Smizanska[71], K. Smolek[127], A.A. Snesarev[95], G. Snidero[75], S. Snyder[25], R. Sobie[170,k], F. Socher[44], A. Soffer[154], D.A. Soh[152,ae], C.A. Solans[30], M. Solar[127], J. Solc[127], E.Yu. Soldatov[97], U. Soldevila[168], E. Solfaroli Camillocci[133a,133b], A.A. Solodkov[129], A. Soloshenko[64], O.V. Solovyanov[129], V. Solovyev[122], P. Sommer[48], H.Y. Song[33b], N. Soni[1], A. Sood[15], A. Sopczak[127], B. Sopko[127], V. Sopko[127], V. Sorin[12], M. Sosebee[8], R. Soualah[165a,165c], P. Soueid[94], A.M. Soukharev[108,c], D. South[42], S. Spagnolo[72a,72b], F. Spanò[76], W.R. Spearman[57], R. Spighi[20a], G. Spigo[30], M. Spousta[128], T. Spreitzer[159], B. Spurlock[8], R.D. St. Denis[53,*], S. Staerz[44], J. Stahlman[121], R. Stamen[58a], E. Stanecka[39], R.W. Stanek[6], C. Stanescu[135a], M. Stanescu-Bellu[42], M.M. Stanitzki[42], S. Stapnes[118], E.A. Starchenko[129], J. Stark[55], P. Staroba[126], P. Starovoitov[42], R. Staszewski[39], P. Stavina[145a,*], P. Steinberg[25], B. Stelzer[143], H.J. Stelzer[30], O. Stelzer-Chilton[160a], H. Stenzel[52], S. Stern[100], G.A. Stewart[53], J.A. Stillings[21], M.C. Stockton[86], M. Stoebe[86], G. Stoicea[26a], P. Stolte[54], S. Stonjek[100], A.R. Stradling[8], A. Straessner[44], M.E. Stramaglia[17], J. Strandberg[148], S. Strandberg[147a,147b], A. Strandlie[118], E. Strauss[144], M. Strauss[112], P. Strizenec[145b], R. Ströhmer[175], D.M. Strom[115], R. Stroynowski[40], S.A. Stucci[17], B. Stugu[14], N.A. Styles[42], D. Su[144], J. Su[124], HS. Subramania[3], R. Subramaniam[78], A. Succurro[12], Y. Sugaya[117], C. Suhr[107], M. Suk[127], V.V. Sulin[95], S. Sultansoy[4c], T. Sumida[67], X. Sun[33a], J.E. Sundermann[48], K. Suruliz[140], G. Susinno[37a,37b], M.R. Sutton[150], Y. Suzuki[65], M. Svatos[126], S. Swedish[169], M. Swiatlowski[144], I. Sykora[145a], T. Sykora[128], D. Ta[89], K. Tackmann[42], J. Taenzer[159], A. Taffard[164], R. Tafirout[160a], N. Taiblum[154],

Y. Takahashi[102], H. Takai[25], R. Takashima[68], H. Takeda[66], T. Takeshita[141], Y. Takubo[65], M. Talby[84], A.A. Talyshev[108,c], J.Y.C. Tam[175], K.G. Tan[87], J. Tanaka[156], R. Tanaka[116], S. Tanaka[132], S. Tanaka[65], A.J. Tanasijczuk[143], K. Tani[66], N. Tannoury[21], S. Tapprogge[82], S. Tarem[153], F. Tarrade[29], G.F. Tartarelli[90a], P. Tas[128], M. Tasevsky[126], T. Tashiro[67], E. Tassi[37a,37b], A. Tavares Delgado[125a,125b], Y. Tayalati[136d], F.E. Taylor[93], G.N. Taylor[87], W. Taylor[160b], F.A. Teischinger[30], M. Teixeira Dias Castanheira[75], P. Teixeira-Dias[76], K.K. Temming[48], H. Ten Kate[30], P.K. Teng[152], J.J. Teoh[117], S. Terada[65], K. Terashi[156], J. Terron[81], S. Terzo[100], M. Testa[47], R.J. Teuscher[159,k], J. Therhaag[21], T. Theveneaux-Pelzer[34], J.P. Thomas[18], J. Thomas-Wilsker[76], E.N. Thompson[35], P.D. Thompson[18], P.D. Thompson[159], R.J. Thompson[83], A.S. Thompson[53], L.A. Thomsen[36], E. Thomson[121], M. Thomson[28], W.M. Thong[87], R.P. Thun[88,*], F. Tian[35], M.J. Tibbetts[15], V.O. Tikhomirov[95,ag], Yu.A. Tikhonov[108,c], S. Timoshenko[97], E. Tiouchichine[84], P. Tipton[177], S. Tisserant[84], T. Todorov[5], S. Todorova-Nova[128], B. Toggerson[7], J. Tojo[69], S. Tokár[145a], K. Tokushuku[65], K. Tollefson[89], L. Tomlinson[83], M. Tomoto[102], L. Tompkins[31], K. Toms[104], N.D. Topilin[64], E. Torrence[115], H. Torres[143], E. Torró Pastor[168], J. Toth[84,ah], F. Touchard[84], D.R. Tovey[140], H.L. Tran[116], T. Trefzger[175], L. Tremblet[30], A. Tricoli[30], I.M. Trigger[160a], S. Trincaz-Duvoid[79], M.F. Tripiana[70], N. Triplett[25], W. Trischuk[159], B. Trocmé[55], C. Troncon[90a], M. Trottier-McDonald[143], M. Trovatelli[135a,135b], P. True[89], M. Trzebinski[39], A. Trzupek[39], C. Tsarouchas[30], J.C-L. Tseng[119], P.V. Tsiareshka[91], D. Tsionou[137], G. Tsipolitis[10], N. Tsirintanis[9], S. Tsiskaridze[12], V. Tsiskaridze[48], E.G. Tskhadadze[51a], I.I. Tsukerman[96], V. Tsulaia[15], S. Tsuno[65], D. Tsybychev[149], A. Tudorache[26a], V. Tudorache[26a], A.N. Tuna[121], S.A. Tupputi[20a,20b], S. Turchikhin[98,af], D. Turecek[127], I. Turk Cakir[4d], R. Turra[90a,90b], P.M. Tuts[35], A. Tykhonov[74], M. Tylmad[147a,147b], M. Tyndel[130], K. Uchida[21], I. Ueda[156], R. Ueno[29], M. Ughetto[84], M. Ugland[14], M. Uhlenbrock[21], F. Ukegawa[161], G. Unal[30], A. Undrus[25], G. Unel[164], F.C. Ungaro[48], Y. Unno[65], C. Unverdorben[99], D. Urbaniec[35], P. Urquijo[87], G. Usai[8], A. Usanova[61], L. Vacavant[84], V. Vacek[127], B. Vachon[86], N. Valencic[106], S. Valentinetti[20a,20b], A. Valero[168], L. Valery[34], S. Valkar[128], E. Valladolid Gallego[168], S. Vallecorsa[49], J.A. Valls Ferrer[168], P.C. Van Der Deijl[106], R. van der Geer[106], H. van der Graaf[106], R. Van Der Leeuw[106], D. van der Ster[30], N. van Eldik[30], P. van Gemmeren[6], J. Van Nieuwkoop[143], I. van Vulpen[106], M.C. van Woerden[30], M. Vanadia[133a,133b], W. Vandelli[30], R. Vanguri[121], A. Vaniachine[6], P. Vankov[42], F. Vannucci[79], G. Vardanyan[178], R. Vari[133a], E.W. Varnes[7], T. Varol[85], D. Varouchas[79], A. Vartapetian[8], K.E. Varvell[151], F. Vazeille[34], T. Vazquez Schroeder[54], J. Veatch[7], F. Veloso[125a,125c], T. Velz[21], S. Veneziano[133a], A. Ventura[72a,72b], D. Ventura[85], M. Venturi[170], N. Venturi[159], A. Venturini[23], V. Vercesi[120a], M. Verducci[139], W. Verkerke[106], J.C. Vermeulen[106], A. Vest[44], M.C. Vetterli[143,e], O. Viazlo[80], I. Vichou[166], T. Vickey[146c,ai], O.E. Vickey Boeriu[146c], G.H.A. Viehhauser[119], S. Viel[169], R. Vigne[30], M. Villa[20a,20b], M. Villaplana Perez[90a,90b], E. Vilucchi[47], M.G. Vincter[29], V.B. Vinogradov[64], J. Virzi[15], I. Vivarelli[150], F. Vives Vaque[3], S. Vlachos[10], D. Vladoiu[99], M. Vlasak[127], A. Vogel[21], M. Vogel[32a], P. Vokac[127], G. Volpi[123a,123b], M. Volpi[87], H. von der Schmitt[100], H. von Radziewski[48], E. von Toerne[21], V. Vorobel[128], K. Vorobev[97], M. Vos[168], R. Voss[30], J.H. Vossebeld[73], N. Vranjes[137], M. Vranjes Milosavljevic[106], V. Vrba[126], M. Vreeswijk[106], T. Vu Anh[48], R. Vuillermet[30], I. Vukotic[31], Z. Vykydal[127], P. Wagner[21], W. Wagner[176], H. Wahlberg[70], S. Wahrmund[44], J. Wakabayashi[102], J. Walder[71], R. Walker[99], W. Walkowiak[142], R. Wall[177], P. Waller[73], B. Walsh[177], C. Wang[152,aj], C. Wang[45], F. Wang[174], H. Wang[15], H. Wang[40], J. Wang[42], J. Wang[33a], K. Wang[86], R. Wang[104], S.M. Wang[152], T. Wang[21], X. Wang[177], C. Wanotayaroj[115], A. Warburton[86], C.P. Ward[28], D.R. Wardrope[77], M. Warsinsky[48], A. Washbrook[46], C. Wasicki[42], I. Watanabe[66], P.M. Watkins[18], A.T. Watson[18], I.J. Watson[151], M.F. Watson[18], G. Watts[139], S. Watts[83], B.M. Waugh[77], S. Webb[83],

JHEP09(2015)049

M.S. Weber[17], S.W. Weber[175], J.S. Webster[31], A.R. Weidberg[119], P. Weigell[100], B. Weinert[60], J. Weingarten[54], C. Weiser[48], H. Weits[106], P.S. Wells[30], T. Wenaus[25], D. Wendland[16], Z. Weng[152,ae], T. Wengler[30], S. Wenig[30], N. Wermes[21], M. Werner[48], P. Werner[30], M. Wessels[58a], J. Wetter[162], K. Whalen[29], A. White[8], M.J. White[1], R. White[32b], S. White[123a,123b], D. Whiteson[164], D. Wicke[176], F.J. Wickens[130], W. Wiedenmann[174], M. Wielers[130], P. Wienemann[21], C. Wiglesworth[36], L.A.M. Wiik-Fuchs[21], P.A. Wijeratne[77], A. Wildauer[100], M.A. Wildt[42,ak], H.G. Wilkens[30], J.Z. Will[99], H.H. Williams[121], S. Williams[28], C. Willis[89], S. Willocq[85], A. Wilson[88], J.A. Wilson[18], I. Wingerter-Seez[5], F. Winklmeier[115], B.T. Winter[21], M. Wittgen[144], T. Wittig[43], J. Wittkowski[99], S.J. Wollstadt[82], M.W. Wolter[39], H. Wolters[125a,125c], B.K. Wosiek[39], J. Wotschack[30], M.J. Woudstra[83], K.W. Wozniak[39], M. Wright[53], M. Wu[55], S.L. Wu[174], X. Wu[49], Y. Wu[88], E. Wulf[35], T.R. Wyatt[83], B.M. Wynne[46], S. Xella[36], M. Xiao[137], D. Xu[33a], L. Xu[33b,al], B. Yabsley[151], S. Yacoob[146b,am], M. Yamada[65], H. Yamaguchi[156], Y. Yamaguchi[156], A. Yamamoto[65], K. Yamamoto[63], S. Yamamoto[156], T. Yamamura[156], T. Yamanaka[156], K. Yamauchi[102], Y. Yamazaki[66], Z. Yan[22], H. Yang[33e], H. Yang[174], U.K. Yang[83], Y. Yang[110], S. Yanush[92], L. Yao[33a], W-M. Yao[15], Y. Yasu[65], E. Yatsenko[42], K.H. Yau Wong[21], J. Ye[40], S. Ye[25], A.L. Yen[57], E. Yildirim[42], M. Yilmaz[4b], R. Yoosoofmiya[124], K. Yorita[172], R. Yoshida[6], K. Yoshihara[156], C. Young[144], C.J.S. Young[30], S. Youssef[22], D.R. Yu[15], J. Yu[8], J.M. Yu[88], J. Yu[113], L. Yuan[66], A. Yurkewicz[107], B. Zabinski[39], R. Zaidan[62], A.M. Zaitsev[129,aa], A. Zaman[149], S. Zambito[23], L. Zanello[133a,133b], D. Zanzi[100], C. Zeitnitz[176], M. Zeman[127], A. Zemla[38a], K. Zengel[23], O. Zenin[129], T. Ženiš[145a], D. Zerwas[116], G. Zevi della Porta[57], D. Zhang[88], F. Zhang[174], H. Zhang[89], J. Zhang[6], L. Zhang[152], X. Zhang[33d], Z. Zhang[116], Z. Zhao[33b], A. Zhemchugov[64], J. Zhong[119], B. Zhou[88], L. Zhou[35], N. Zhou[164], C.G. Zhu[33d], H. Zhu[33a], J. Zhu[88], Y. Zhu[33b], X. Zhuang[33a], A. Zibell[175], D. Zieminska[60], N.I. Zimine[64], C. Zimmermann[82], R. Zimmermann[21], S. Zimmermann[21], S. Zimmermann[48], Z. Zinonos[54], M. Ziolkowski[142], G. Zobernig[174], A. Zoccoli[20a,20b], M. zur Nedden[16], G. Zurzolo[103a,103b], V. Zutshi[107], L. Zwalinski[30]

[1] Department of Physics, University of Adelaide, Adelaide, Australia
[2] Physics Department, SUNY Albany, Albany NY, United States of America
[3] Department of Physics, University of Alberta, Edmonton AB, Canada
[4] [(a)] Department of Physics, Ankara University, Ankara; [(b)] Department of Physics, Gazi University, Ankara; [(c)] Division of Physics, TOBB University of Economics and Technology, Ankara; [(d)] Turkish Atomic Energy Authority, Ankara, Turkey
[5] LAPP, CNRS/IN2P3 and Université de Savoie, Annecy-le-Vieux, France
[6] High Energy Physics Division, Argonne National Laboratory, Argonne IL, United States of America
[7] Department of Physics, University of Arizona, Tucson AZ, United States of America
[8] Department of Physics, The University of Texas at Arlington, Arlington TX, United States of America
[9] Physics Department, University of Athens, Athens, Greece
[10] Physics Department, National Technical University of Athens, Zografou, Greece
[11] Institute of Physics, Azerbaijan Academy of Sciences, Baku, Azerbaijan
[12] Institut de Física d'Altes Energies and Departament de Física de la Universitat Autònoma de Barcelona, Barcelona, Spain
[13] [(a)] Institute of Physics, University of Belgrade, Belgrade; [(b)] Vinca Institute of Nuclear Sciences, University of Belgrade, Belgrade, Serbia
[14] Department for Physics and Technology, University of Bergen, Bergen, Norway
[15] Physics Division, Lawrence Berkeley National Laboratory and University of California, Berkeley CA, United States of America
[16] Department of Physics, Humboldt University, Berlin, Germany
[17] Albert Einstein Center for Fundamental Physics and Laboratory for High Energy Physics, University of Bern, Bern, Switzerland

JHEP09(2015)049

[18] School of Physics and Astronomy, University of Birmingham, Birmingham, United Kingdom
[19] [(a)] Department of Physics, Bogazici University, Istanbul; [(b)] Department of Physics, Dogus University, Istanbul; [(c)] Department of Physics Engineering, Gaziantep University, Gaziantep, Turkey
[20] [(a)] INFN Sezione di Bologna; [(b)] Dipartimento di Fisica e Astronomia, Università di Bologna, Bologna, Italy
[21] Physikalisches Institut, University of Bonn, Bonn, Germany
[22] Department of Physics, Boston University, Boston MA, United States of America
[23] Department of Physics, Brandeis University, Waltham MA, United States of America
[24] [(a)] Universidade Federal do Rio De Janeiro COPPE/EE/IF, Rio de Janeiro; [(b)] Electrical Circuits Department, Federal University of Juiz de Fora (UFJF), Juiz de Fora; [(c)] Federal University of Sao Joao del Rei (UFSJ), Sao Joao del Rei; [(d)] Instituto de Fisica, Universidade de Sao Paulo, Sao Paulo, Brazil
[25] Physics Department, Brookhaven National Laboratory, Upton NY, United States of America
[26] [(a)] National Institute of Physics and Nuclear Engineering, Bucharest; [(b)] National Institute for Research and Development of Isotopic and Molecular Technologies, Physics Department, Cluj Napoca; [(c)] University Politehnica Bucharest, Bucharest; [(d)] West University in Timisoara, Timisoara, Romania
[27] Departamento de Física, Universidad de Buenos Aires, Buenos Aires, Argentina
[28] Cavendish Laboratory, University of Cambridge, Cambridge, United Kingdom
[29] Department of Physics, Carleton University, Ottawa ON, Canada
[30] CERN, Geneva, Switzerland
[31] Enrico Fermi Institute, University of Chicago, Chicago IL, United States of America
[32] [(a)] Departamento de Física, Pontificia Universidad Católica de Chile, Santiago; [(b)] Departamento de Física, Universidad Técnica Federico Santa María, Valparaíso, Chile
[33] [(a)] Institute of High Energy Physics, Chinese Academy of Sciences, Beijing; [(b)] Department of Modern Physics, University of Science and Technology of China, Anhui; [(c)] Department of Physics, Nanjing University, Jiangsu; [(d)] School of Physics, Shandong University, Shandong; [(e)] Physics Department, Shanghai Jiao Tong University, Shanghai, China
[34] Laboratoire de Physique Corpusculaire, Clermont Université and Université Blaise Pascal and CNRS/IN2P3, Clermont-Ferrand, France
[35] Nevis Laboratory, Columbia University, Irvington NY, United States of America
[36] Niels Bohr Institute, University of Copenhagen, Kobenhavn, Denmark
[37] [(a)] INFN Gruppo Collegato di Cosenza, Laboratori Nazionali di Frascati; [(b)] Dipartimento di Fisica, Università della Calabria, Rende, Italy
[38] [(a)] AGH University of Science and Technology, Faculty of Physics and Applied Computer Science, Krakow; [(b)] Marian Smoluchowski Institute of Physics, Jagiellonian University, Krakow, Poland
[39] The Henryk Niewodniczanski Institute of Nuclear Physics, Polish Academy of Sciences, Krakow, Poland
[40] Physics Department, Southern Methodist University, Dallas TX, United States of America
[41] Physics Department, University of Texas at Dallas, Richardson TX, United States of America
[42] DESY, Hamburg and Zeuthen, Germany
[43] Institut für Experimentelle Physik IV, Technische Universität Dortmund, Dortmund, Germany
[44] Institut für Kern- und Teilchenphysik, Technische Universität Dresden, Dresden, Germany
[45] Department of Physics, Duke University, Durham NC, United States of America
[46] SUPA - School of Physics and Astronomy, University of Edinburgh, Edinburgh, United Kingdom
[47] INFN Laboratori Nazionali di Frascati, Frascati, Italy
[48] Fakultät für Mathematik und Physik, Albert-Ludwigs-Universität, Freiburg, Germany
[49] Section de Physique, Université de Genève, Geneva, Switzerland
[50] [(a)] INFN Sezione di Genova; [(b)] Dipartimento di Fisica, Università di Genova, Genova, Italy
[51] [(a)] E. Andronikashvili Institute of Physics, Iv. Javakhishvili Tbilisi State University, Tbilisi; [(b)] High Energy Physics Institute, Tbilisi State University, Tbilisi, Georgia

JHEP09(2015)049

[52] II Physikalisches Institut, Justus-Liebig-Universität Giessen, Giessen, Germany
[53] SUPA - School of Physics and Astronomy, University of Glasgow, Glasgow, United Kingdom
[54] II Physikalisches Institut, Georg-August-Universität, Göttingen, Germany
[55] Laboratoire de Physique Subatomique et de Cosmologie, Université Grenoble-Alpes, CNRS/IN2P3, Grenoble, France
[56] Department of Physics, Hampton University, Hampton VA, United States of America
[57] Laboratory for Particle Physics and Cosmology, Harvard University, Cambridge MA, United States of America
[58] [(a)] Kirchhoff-Institut für Physik, Ruprecht-Karls-Universität Heidelberg, Heidelberg; [(b)] Physikalisches Institut, Ruprecht-Karls-Universität Heidelberg, Heidelberg; [(c)] ZITI Institut für technische Informatik, Ruprecht-Karls-Universität Heidelberg, Mannheim, Germany
[59] Faculty of Applied Information Science, Hiroshima Institute of Technology, Hiroshima, Japan
[60] Department of Physics, Indiana University, Bloomington IN, United States of America
[61] Institut für Astro- und Teilchenphysik, Leopold-Franzens-Universität, Innsbruck, Austria
[62] University of Iowa, Iowa City IA, United States of America
[63] Department of Physics and Astronomy, Iowa State University, Ames IA, United States of America
[64] Joint Institute for Nuclear Research, JINR Dubna, Dubna, Russia
[65] KEK, High Energy Accelerator Research Organization, Tsukuba, Japan
[66] Graduate School of Science, Kobe University, Kobe, Japan
[67] Faculty of Science, Kyoto University, Kyoto, Japan
[68] Kyoto University of Education, Kyoto, Japan
[69] Department of Physics, Kyushu University, Fukuoka, Japan
[70] Instituto de Física La Plata, Universidad Nacional de La Plata and CONICET, La Plata, Argentina
[71] Physics Department, Lancaster University, Lancaster, United Kingdom
[72] [(a)] INFN Sezione di Lecce; [(b)] Dipartimento di Matematica e Fisica, Università del Salento, Lecce, Italy
[73] Oliver Lodge Laboratory, University of Liverpool, Liverpool, United Kingdom
[74] Department of Physics, Jožef Stefan Institute and University of Ljubljana, Ljubljana, Slovenia
[75] School of Physics and Astronomy, Queen Mary University of London, London, United Kingdom
[76] Department of Physics, Royal Holloway University of London, Surrey, United Kingdom
[77] Department of Physics and Astronomy, University College London, London, United Kingdom
[78] Louisiana Tech University, Ruston LA, United States of America
[79] Laboratoire de Physique Nucléaire et de Hautes Energies, UPMC and Université Paris-Diderot and CNRS/IN2P3, Paris, France
[80] Fysiska institutionen, Lunds universitet, Lund, Sweden
[81] Departamento de Fisica Teorica C-15, Universidad Autonoma de Madrid, Madrid, Spain
[82] Institut für Physik, Universität Mainz, Mainz, Germany
[83] School of Physics and Astronomy, University of Manchester, Manchester, United Kingdom
[84] CPPM, Aix-Marseille Université and CNRS/IN2P3, Marseille, France
[85] Department of Physics, University of Massachusetts, Amherst MA, United States of America
[86] Department of Physics, McGill University, Montreal QC, Canada
[87] School of Physics, University of Melbourne, Victoria, Australia
[88] Department of Physics, The University of Michigan, Ann Arbor MI, United States of America
[89] Department of Physics and Astronomy, Michigan State University, East Lansing MI, United States of America
[90] [(a)] INFN Sezione di Milano; [(b)] Dipartimento di Fisica, Università di Milano, Milano, Italy
[91] B.I. Stepanov Institute of Physics, National Academy of Sciences of Belarus, Minsk, Republic of Belarus
[92] National Scientific and Educational Centre for Particle and High Energy Physics, Minsk, Republic of Belarus
[93] Department of Physics, Massachusetts Institute of Technology, Cambridge MA, United States of America

JHEP09(2015)049

[94] Group of Particle Physics, University of Montreal, Montreal QC, Canada
[95] P.N. Lebedev Institute of Physics, Academy of Sciences, Moscow, Russia
[96] Institute for Theoretical and Experimental Physics (ITEP), Moscow, Russia
[97] National Research Nuclear University MEPhI, Moscow, Russia
[98] D.V. Skobeltsyn Institute of Nuclear Physics, M.V. Lomonosov Moscow State University, Moscow, Russia
[99] Fakultät für Physik, Ludwig-Maximilians-Universität München, München, Germany
[100] Max-Planck-Institut für Physik (Werner-Heisenberg-Institut), München, Germany
[101] Nagasaki Institute of Applied Science, Nagasaki, Japan
[102] Graduate School of Science and Kobayashi-Maskawa Institute, Nagoya University, Nagoya, Japan
[103] [(a)] INFN Sezione di Napoli; [(b)] Dipartimento di Fisica, Università di Napoli, Napoli, Italy
[104] Department of Physics and Astronomy, University of New Mexico, Albuquerque NM, United States of America
[105] Institute for Mathematics, Astrophysics and Particle Physics, Radboud University Nijmegen/Nikhef, Nijmegen, Netherlands
[106] Nikhef National Institute for Subatomic Physics and University of Amsterdam, Amsterdam, Netherlands
[107] Department of Physics, Northern Illinois University, DeKalb IL, United States of America
[108] Budker Institute of Nuclear Physics, SB RAS, Novosibirsk, Russia
[109] Department of Physics, New York University, New York NY, United States of America
[110] Ohio State University, Columbus OH, United States of America
[111] Faculty of Science, Okayama University, Okayama, Japan
[112] Homer L. Dodge Department of Physics and Astronomy, University of Oklahoma, Norman OK, United States of America
[113] Department of Physics, Oklahoma State University, Stillwater OK, United States of America
[114] Palacký University, RCPTM, Olomouc, Czech Republic
[115] Center for High Energy Physics, University of Oregon, Eugene OR, United States of America
[116] LAL, Université Paris-Sud and CNRS/IN2P3, Orsay, France
[117] Graduate School of Science, Osaka University, Osaka, Japan
[118] Department of Physics, University of Oslo, Oslo, Norway
[119] Department of Physics, Oxford University, Oxford, United Kingdom
[120] [(a)] INFN Sezione di Pavia; [(b)] Dipartimento di Fisica, Università di Pavia, Pavia, Italy
[121] Department of Physics, University of Pennsylvania, Philadelphia PA, United States of America
[122] Petersburg Nuclear Physics Institute, Gatchina, Russia
[123] [(a)] INFN Sezione di Pisa; [(b)] Dipartimento di Fisica E. Fermi, Università di Pisa, Pisa, Italy
[124] Department of Physics and Astronomy, University of Pittsburgh, Pittsburgh PA, United States of America
[125] [(a)] Laboratorio de Instrumentacao e Fisica Experimental de Particulas - LIP, Lisboa; [(b)] Faculdade de Ciências, Universidade de Lisboa, Lisboa; [(c)] Department of Physics, University of Coimbra, Coimbra; [(d)] Centro de Física Nuclear da Universidade de Lisboa, Lisboa; [(e)] Departamento de Fisica, Universidade do Minho, Braga; [(f)] Departamento de Fisica Teorica y del Cosmos and CAFPE, Universidad de Granada, Granada (Spain); [(g)] Dep Fisica and CEFITEC of Faculdade de Ciencias e Tecnologia, Universidade Nova de Lisboa, Caparica, Portugal
[126] Institute of Physics, Academy of Sciences of the Czech Republic, Praha, Czech Republic
[127] Czech Technical University in Prague, Praha, Czech Republic
[128] Faculty of Mathematics and Physics, Charles University in Prague, Praha, Czech Republic
[129] State Research Center Institute for High Energy Physics, Protvino, Russia
[130] Particle Physics Department, Rutherford Appleton Laboratory, Didcot, United Kingdom
[131] Physics Department, University of Regina, Regina SK, Canada
[132] Ritsumeikan University, Kusatsu, Shiga, Japan
[133] [(a)] INFN Sezione di Roma; [(b)] Dipartimento di Fisica, Sapienza Università di Roma, Roma, Italy
[134] [(a)] INFN Sezione di Roma Tor Vergata; [(b)] Dipartimento di Fisica, Università di Roma Tor Vergata, Roma, Italy

JHEP09(2015)049

135 [a] INFN Sezione di Roma Tre; [b] Dipartimento di Matematica e Fisica, Università Roma Tre, Roma, Italy
136 [a] Faculté des Sciences Ain Chock, Réseau Universitaire de Physique des Hautes Energies - Université Hassan II, Casablanca; [b] Centre National de l'Energie des Sciences Techniques Nucleaires, Rabat; [c] Faculté des Sciences Semlalia, Université Cadi Ayyad, LPHEA-Marrakech; [d] Faculté des Sciences, Université Mohamed Premier and LPTPM, Oujda; [e] Faculté des sciences, Université Mohammed V-Agdal, Rabat, Morocco
137 DSM/IRFU (Institut de Recherches sur les Lois Fondamentales de l'Univers), CEA Saclay (Commissariat à l'Energie Atomique et aux Energies Alternatives), Gif-sur-Yvette, France
138 Santa Cruz Institute for Particle Physics, University of California Santa Cruz, Santa Cruz CA, United States of America
139 Department of Physics, University of Washington, Seattle WA, United States of America
140 Department of Physics and Astronomy, University of Sheffield, Sheffield, United Kingdom
141 Department of Physics, Shinshu University, Nagano, Japan
142 Fachbereich Physik, Universität Siegen, Siegen, Germany
143 Department of Physics, Simon Fraser University, Burnaby BC, Canada
144 SLAC National Accelerator Laboratory, Stanford CA, United States of America
145 [a] Faculty of Mathematics, Physics & Informatics, Comenius University, Bratislava; [b] Department of Subnuclear Physics, Institute of Experimental Physics of the Slovak Academy of Sciences, Kosice, Slovak Republic
146 [a] Department of Physics, University of Cape Town, Cape Town; [b] Department of Physics, University of Johannesburg, Johannesburg; [c] School of Physics, University of the Witwatersrand, Johannesburg, South Africa
147 [a] Department of Physics, Stockholm University; [b] The Oskar Klein Centre, Stockholm, Sweden
148 Physics Department, Royal Institute of Technology, Stockholm, Sweden
149 Departments of Physics & Astronomy and Chemistry, Stony Brook University, Stony Brook NY, United States of America
150 Department of Physics and Astronomy, University of Sussex, Brighton, United Kingdom
151 School of Physics, University of Sydney, Sydney, Australia
152 Institute of Physics, Academia Sinica, Taipei, Taiwan
153 Department of Physics, Technion: Israel Institute of Technology, Haifa, Israel
154 Raymond and Beverly Sackler School of Physics and Astronomy, Tel Aviv University, Tel Aviv, Israel
155 Department of Physics, Aristotle University of Thessaloniki, Thessaloniki, Greece
156 International Center for Elementary Particle Physics and Department of Physics, The University of Tokyo, Tokyo, Japan
157 Graduate School of Science and Technology, Tokyo Metropolitan University, Tokyo, Japan
158 Department of Physics, Tokyo Institute of Technology, Tokyo, Japan
159 Department of Physics, University of Toronto, Toronto ON, Canada
160 [a] TRIUMF, Vancouver BC; [b] Department of Physics and Astronomy, York University, Toronto ON, Canada
161 Faculty of Pure and Applied Sciences, University of Tsukuba, Tsukuba, Japan
162 Department of Physics and Astronomy, Tufts University, Medford MA, United States of America
163 Centro de Investigaciones, Universidad Antonio Narino, Bogota, Colombia
164 Department of Physics and Astronomy, University of California Irvine, Irvine CA, United States of America
165 [a] INFN Gruppo Collegato di Udine, Sezione di Trieste, Udine; [b] ICTP, Trieste; [c] Dipartimento di Chimica, Fisica e Ambiente, Università di Udine, Udine, Italy
166 Department of Physics, University of Illinois, Urbana IL, United States of America
167 Department of Physics and Astronomy, University of Uppsala, Uppsala, Sweden
168 Instituto de Física Corpuscular (IFIC) and Departamento de Física Atómica, Molecular y Nuclear and Departamento de Ingeniería Electrónica and Instituto de Microelectrónica de Barcelona (IMB-CNM), University of Valencia and CSIC, Valencia, Spain

[169] Department of Physics, University of British Columbia, Vancouver BC, Canada
[170] Department of Physics and Astronomy, University of Victoria, Victoria BC, Canada
[171] Department of Physics, University of Warwick, Coventry, United Kingdom
[172] Waseda University, Tokyo, Japan
[173] Department of Particle Physics, The Weizmann Institute of Science, Rehovot, Israel
[174] Department of Physics, University of Wisconsin, Madison WI, United States of America
[175] Fakultät für Physik und Astronomie, Julius-Maximilians-Universität, Würzburg, Germany
[176] Fachbereich C Physik, Bergische Universität Wuppertal, Wuppertal, Germany
[177] Department of Physics, Yale University, New Haven CT, United States of America
[178] Yerevan Physics Institute, Yerevan, Armenia
[179] Centre de Calcul de l'Institut National de Physique Nucléaire et de Physique des Particules (IN2P3), Villeurbanne, France

[a] Also at Department of Physics, King's College London, London, United Kingdom
[b] Also at Institute of Physics, Azerbaijan Academy of Sciences, Baku, Azerbaijan
[c] Also at Novosibirsk State University, Novosibirsk, Russia
[d] Also at Particle Physics Department, Rutherford Appleton Laboratory, Didcot, United Kingdom
[e] Also at TRIUMF, Vancouver BC, Canada
[f] Also at Department of Physics, California State University, Fresno CA, United States of America
[g] Also at Department of Physics, University of Fribourg, Fribourg, Switzerland
[h] Also at Tomsk State University, Tomsk, Russia
[i] Also at CPPM, Aix-Marseille Université and CNRS/IN2P3, Marseille, France
[j] Also at Università di Napoli Parthenope, Napoli, Italy
[k] Also at Institute of Particle Physics (IPP), Canada
[l] Also at Department of Physics, St. Petersburg State Polytechnical University, St. Petersburg, Russia
[m] Also at Chinese University of Hong Kong, China
[n] Also at Louisiana Tech University, Ruston LA, United States of America
[o] Also at Institucio Catalana de Recerca i Estudis Avancats, ICREA, Barcelona, Spain
[p] Also at Department of Physics, The University of Texas at Austin, Austin TX, United States of America
[q] Also at Institute of Theoretical Physics, Ilia State University, Tbilisi, Georgia
[r] Also at CERN, Geneva, Switzerland
[s] Also at Ochadai Academic Production, Ochanomizu University, Tokyo, Japan
[t] Also at Manhattan College, New York NY, United States of America
[u] Also at Institute of Physics, Academia Sinica, Taipei, Taiwan
[v] Also at LAL, Université Paris-Sud and CNRS/IN2P3, Orsay, France
[w] Also at Academia Sinica Grid Computing, Institute of Physics, Academia Sinica, Taipei, Taiwan
[x] Also at Laboratoire de Physique Nucléaire et de Hautes Energies, UPMC and Université Paris-Diderot and CNRS/IN2P3, Paris, France
[y] Also at School of Physical Sciences, National Institute of Science Education and Research, Bhubaneswar, India
[z] Also at Dipartimento di Fisica, Sapienza Università di Roma, Roma, Italy
[aa] Also at Moscow Institute of Physics and Technology State University, Dolgoprudny, Russia
[ab] Also at section de Physique, Université de Genève, Geneva, Switzerland
[ac] Also at International School for Advanced Studies (SISSA), Trieste, Italy
[ad] Also at Department of Physics and Astronomy, University of South Carolina, Columbia SC, United States of America
[ae] Also at School of Physics and Engineering, Sun Yat-sen University, Guangzhou, China
[af] Also at Faculty of Physics, M.V.Lomonosov Moscow State University, Moscow, Russia
[ag] Also at National Research Nuclear University MEPhI, Moscow, Russia
[ah] Also at Institute for Particle and Nuclear Physics, Wigner Research Centre for Physics, Budapest, Hungary

JHEP09(2015)049

[ai] Also at Department of Physics, Oxford University, Oxford, United Kingdom
[aj] Also at Department of Physics, Nanjing University, Jiangsu, China
[ak] Also at Institut für Experimentalphysik, Universität Hamburg, Hamburg, Germany
[al] Also at Department of Physics, The University of Michigan, Ann Arbor MI, United States of America
[am] Also at Discipline of Physics, University of KwaZulu-Natal, Durban, South Africa
[*] Deceased

JHEP09(2015)049